Chapter 4
Radioactive Decays

4.1 Introduction

Decays are a category of reaction where a particle, or a nucleus, transforms into two or more particles or nuclei. We have already introduced the α-, β- and γ-emitting decays. In the α decay (Fig. 4.1), the parent nucleus emits an α particle, which is a nucleus of ${}^4_2\mathrm{He}$, and the resulting daughter nucleus has an atomic number which is two units lower and a mass number which is four units lower. In the β decay (Fig. 4.2), an electron or a positron is emitted, and the resulting daughter nucleus has an atomic number lower by one unit, while the mass number remains unchanged (Table 4.1).

The γ radiation is emitted by nuclei which are in an excited state and no change in their composition occurs. Typically, nuclei are in an excited state after α or β decays, so the γ radiation is associated with the other two.

In all decays, the 4-momentum is conserved. We recall that we indicate with A the total number of nucleons and with Z the number of protons, so the pair (A, Z) uniquely identifies a nuclide. For α decays, we have (Fig. 4.3)

$$(A, Z) \rightarrow (A-4, Z-2) + \alpha. \tag{4.1}$$

In the rest frame of the parent nucleus, the α particle and the daughter nucleus recoil back to back, with the same momentum. The energy states of nuclei have discrete values, and these two conditions explain why, for a given nuclide and a given daughter, the α particles emitted have all the same energy.

With the same conditions, the continuous spectrum of the $\beta^{\pm}$ decay seems to defy the conservation of 4-momentum:

$$\beta^{\pm}\text{decay } (A, Z) \rightarrow (A, Z \mp 1) + \beta^{\pm} \text{ (missing a term)} \tag{4.2}$$

S. D'Auria, *Introduction to Nuclear and Particle Physics*,
Undergraduate Lecture Notes in Physics,
https://doi.org/10.1007/978-3-319-93855-4_4

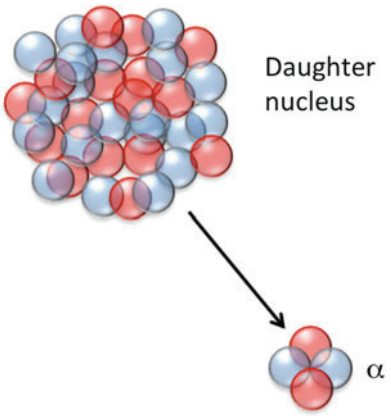

Fig. 4.1 Schematic representation of the emission of an alpha particle, which is a nucleus of helium, or a bound state of two protons and two neutrons

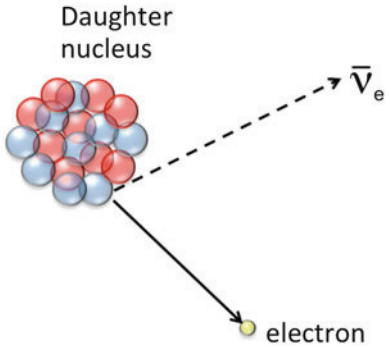

Fig. 4.2 Representation of a beta decay. Note the emission of a (anti)-neutrino: it is a 3-body decay

Table 4.1 Table of the nuclear transmutation due to α and β decays

Decay	Parent	Daughter
α	(A, Z)	$(A-4, Z-2)$
β^-	(A, Z)	$(A, Z+1)$
β^+	(A, Z)	$(A, Z-1)$
γ	(A, Z)	(A, Z)

Also in this case, we would expect the electron or positron to recoil against the nucleus and have only one value of momentum, or just a restricted range of momenta, to account for a natural "width", of quantum origin. This puzzle led Wolfgang Pauli to make the hypothesis that another neutral particle is emitted and is not detected experimentally. He called the particle *neutron*, but the discovery of what we now call a neutron led Enrico Fermi to call this particle *neutrino*, for "the little neutral" particle. It is indicated with ν_e; the subscript e will be clearer later.

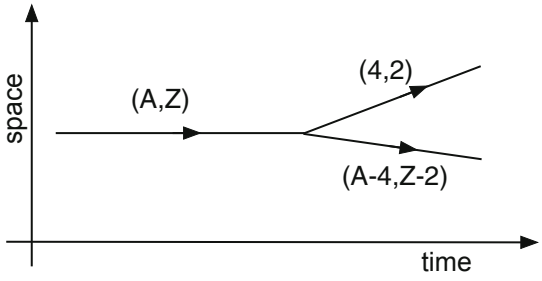

Fig. 4.3 This diagram in the $x - t$ plane illustrates the α decay of a nucleus: $(A, Z) \rightarrow (A-4, Z-2) + \alpha$

Only 30 years later, the neutrino was detected experimentally. The correct decay reaction is

$$\beta^{\pm}\text{decay } (A, Z) \rightarrow (A, Z \mp 1) + \beta^{\pm} + \nu_e \tag{4.3}$$

In order for a decay to occur, the final state must be energetically allowed. The energy must be conserved, so the sum of total energy of the final state, including the kinetic energy, must be equal to the total energy of the initial particle or nucleus, but this will be the topic in the last chapter of this book.

4.2 The Laws of Radioactive Decay

Independently of the mechanism and type of decay, we'll introduce now some general considerations that apply to all types of decays and derive the law of the time evolution of radioactive decays.

The physics of decays is the same in every reference frame. There is one frame which makes calculations easy, and it is the frame where the initial particle is at rest.

We can have two pictures: one is the one-particle picture of the decay; we pick up one particle and after a time, which is random, we observe it to decay. We also have the opportunity to repeat the experiment N times, with N particle of identical type and nature; we see that the decay times are distributed according to a mathematical function.

In the single particle picture, the basic assumption we can make is that the probability of the decay to occur within the *small* time interval Δt is constant in time; it does not depend on time at all. Of course, the larger is the *small* time interval in which we observe, the larger is the probability dP to decay. It is natural to assume that, for small, but finite, intervals Δt, the probability to decay is just proportional to the time.

$$dP = \lambda dt = \frac{1}{\tau_0} dt \ . \tag{4.4}$$

The constant λ must have physical dimensions $[T^{-1}]$, and it is called *decay rate*, while $1/\lambda = \tau_0$ is the *mean lifetime* or simply *lifetime*. Suppose we have N_0 radioactive nuclei at rest at time t_0. Then, Eq. (4.4) applies to each of them. We can recall the frequentist definition of probability, as the relative frequency of an event, i.e. the ratio between the number of times a certain event occurred and the number of times that it was possible that the event occurred, in the limit of a large number of tries. We observe for a *small* time Δt a very large number N_0 of initial nuclei; this is our number of tries, because each of them could decay. Out of those, we observe a small number N_d decay:

$$dP = \frac{N_d}{N_0} = \frac{\Delta t}{\tau_0} \tag{4.5}$$

for the number of decays N_d. We now want to know the variation of the number N of initial nuclei or particles: $\Delta N = -N_d$. Substituting in Eq. (4.5), we have

$$\frac{\Delta N}{\Delta t} = -\frac{N}{\tau_0} \tag{4.6}$$

(note the minus sign) which is valid at any time. At the limit of infinitesimal time interval $\Delta t \to dt$, we obtain

$$\frac{dN}{dt} = -\frac{N}{\tau_0}\,, \tag{4.7}$$

which we can consider as a differential equation for the number of nuclei, or particles, which are still undecayed at the time t, i.e. the function $N(t)$. The solution is

$$N(t) = N_0 e^{-t/\tau_0} \tag{4.8}$$

This formula fits extremely well the experimental measurements. An example is shown in Fig. 4.4

We can verify that

$$\frac{d}{dt}N(t) = -\frac{1}{\tau_0}N_0 e^{-t/\tau_0} = -\frac{N(t)}{\tau_0}$$

Suppose we have a radiation detector next to our radiation source (Fig. 4.5). In general, it will detect and count only a fraction ϵ of the radiation emitted due to an intrinsic detection efficiency and to geometrical acceptance. The counting rate R will be proportional to the *activity* $\mathcal{A}$ of the source:

$$R = \epsilon\mathcal{A} = \epsilon(-dN/dt) = \epsilon\lambda N(t)$$

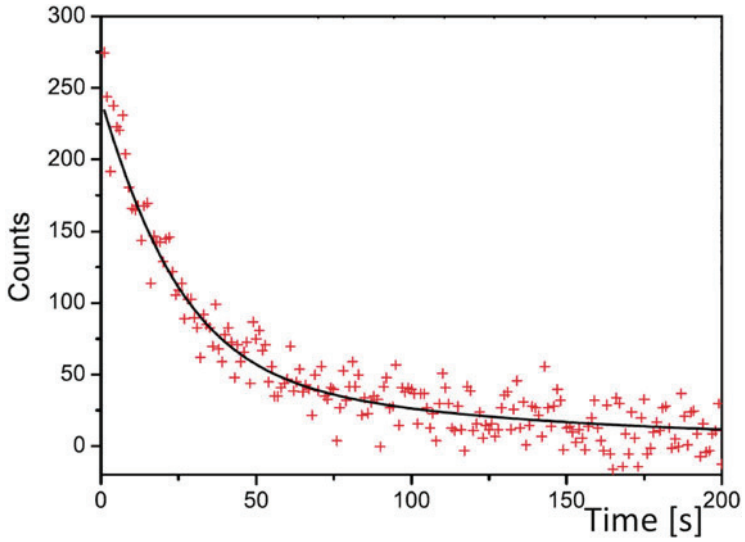

Fig. 4.4 Experimental decay curve of the nuclide ^{229}Rn, a beta emitter discovered in 2009. From D. Neidherr et al., Phys. Rev. Lett. 102 (2009)

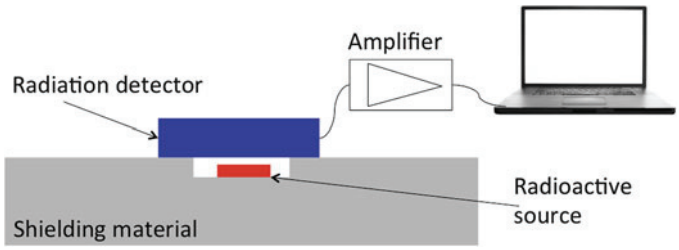

Fig. 4.5 A particle *detector* is used to measure the activity of a radioactive source. In this case, only about 50% of the emitted radiation can reach the detector. In addition, especially in case of γ radiation, some radiation may escape detection, contributing to inefficiency, which must be taken into account to calculate the real activity of the source

So, the activity of the source at time t is

$$\mathcal{A}(t) = \lambda N(t) = \frac{1}{\tau} N(t) = \frac{1}{\tau\epsilon} R(t) \tag{4.9}$$

The activity of a radioactive source (or material) is measured in *Becquerel (Bq)*, which corresponds to one decay per second. Its physical dimensions are $[T^{-1}]$. A radioactive source of 1 Bq, if measured with a perfect detector, will give a count rate of 1 Hz. Of course, the normal multiple and sub-multiples of this unit are also used. Another unit for the activity, which is not an SI unit, is the *Curie* (Ci), a practical unit which is defined from the activity of one gram of ^{226}Ra : 37 MBq= 1 mCi. From Eq. (4.8), it is evident that the activity of a radioactive source decreases

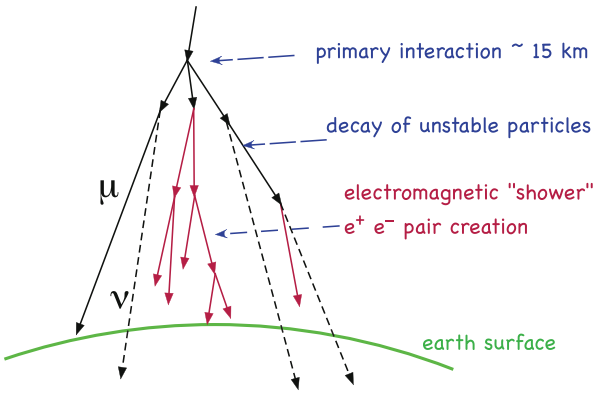

Fig. 4.6 Cosmic rays are high-energy particles coming from the space. They start interacting with the outer layers of the atmosphere, generating cosmic-ray showers

exponentially with time. The average lifetime of a nuclide or particle is the time occurring to reduce to a fraction $1/e = 0.368$ of the initial sample. Often, it is given the *half-life*, which is the time occurring to a sample to half its initial radioactivity. The two values are related by $\log(2)$.

So far, we have considered that the nuclei are always at rest with respect to the laboratory. This is not always the case for elementary particles, or exotic nuclei. An elementary particle which we call *muon* ($\mu^{\pm}$) has a mean lifetime of 2.197 μs when it is at rest in the lab. It is produced copiously by cosmic rays at the top of the atmosphere, say at 30 to 15 km from the Earth surface (Fig. 4.6). At the speed of light, it would take 100 μs to reach the Earth's surface, and this time is much larger than the muon lifetime. However, as time is dilated by relativistic effects, the muon lifetime, as measured in the laboratory reference frame, is increased by a factor $\gamma(v)$. So, we are constantly bombarded by muons from cosmic rays.

4.3 More on Radioactive Decays

The radioactive decay is a particular kind of nuclear reaction, where a species "A" decays into two or more *decay products* (B, C, D). Some typical examples are the alpha decay:

$$^{241}\mathrm{Am} \rightarrow ^{237}\mathrm{Np} + \alpha(5.49\ \mathrm{MeV}) \tag{4.10}$$

a beta decay:

$$^{90}\mathrm{Sr} \rightarrow ^{90}\mathrm{Y} + \beta^{-} + \overline{\nu_e} \tag{4.11}$$

and a gamma decay:

$$^{99m}\mathrm{Tc}^{*} \rightarrow ^{99}\mathrm{Tc} + \gamma(140\ \mathrm{keV}) \tag{4.12}$$

The gamma decay is rather a transition between two *isomers* of the same nuclide, with emission of energy. We have also mentioned an elementary particle, the muon $\mu^{\pm}$, it decays

$$\mu^- \rightarrow e^- + \nu_\mu + \overline{\nu_e} \tag{4.13}$$

with a mean lifetime of 2.197 μs.

There is one reference frame, where the initial particle, which is also called the "parent", is at rest. In this frame, the decay mean lifetime is minimum and is a characteristic of the decay.

For some nuclides, or elementary particles, two or more decay channels may be open: for example, a nucleus can undergo both α and β decay. We say that there is a *branching*, and we can write the probability for a nucleus to undergo α decay in the time dt as:

$$dP_\alpha = \lambda_\alpha dt \tag{4.14}$$

and we can write something similar for the β decay:

$$dP_\beta = \lambda_\beta dt \tag{4.15}$$

then the total probability to decay in either mode is

$$P_{\text{tot}} = (\lambda_\alpha + \lambda_\beta)dt \tag{4.16}$$

and therefore

$$\frac{dN}{dt} = -(\lambda_\alpha + \lambda_\beta)N \tag{4.17}$$

The *average lifetime* of the given nuclide has only one value:

$$\tau = \frac{1}{\lambda_\alpha + \lambda_\beta} \tag{4.18}$$

The α *Branching Ratio* ($\mathcal{BR}$) is the ratio of the number of alpha decays to the total number of decays in a given time:

$$\mathcal{BR}(\alpha) = \frac{\lambda_\alpha}{\lambda_\alpha + \lambda_\beta} \tag{4.19}$$

An example in nuclear physics is

$$^{213}\text{Bi} \rightarrow ^{213}\text{Po} + \beta^- + \overline{\nu}_e \qquad 1.423\ \text{MeV}(97.8\%) \tag{4.20}$$

$$^{213}\text{Bi} \rightarrow ^{209}\text{Tl} + \alpha \qquad 5.87\ \text{MeV}(2.20\%) \tag{4.21}$$

Table 4.2 The main decay modes of the particle Z^0, with the corresponding branching fractions

Decay	Mode	Fraction (%)
Γ_1	$e^+ e^-$	(3.363 ± 0.004)
Γ_2	$\mu^+ \mu^-$	(3.366 ± 0.007)
Γ_3	$\tau^+ \tau^-$	(3.367 ± 0.008)
Γ_4	$\ell^+ \ell^-$	(3.3658 ± 0.0023)
Γ_5	Invisible	(20.00 ± 0.06)
Γ_6	Hadrons	(69.91 ± 0.06)
Γ_9	$c\,\overline{c}$	(12.03 ± 0.21)
Γ_{10}	$b\,\overline{b}$	(15.12 ± 0.05)

As an example: the decay $Z^0 \rightarrow e^+e^-$ occurs with a branching fraction of 3.36%. The branching fractions above add up to more than 100% because they are not exclusive: ℓ indicates any of the e, μ, τ particles, and $c\,\overline{c}$ and $b\,\overline{b}$ are also included in the decay to "hadrons". All these particles will be more familiar in Chap. 6. Data from the Particle Data Group

An example in particle physics is the decay of the particle Z^0, as shown in Table 4.2.

In a simple decay $A \rightarrow B + C$, the products B and C are stable. However, a decay product B can itself be a radioactive nuclide, or an unstable particle. In this case, we have a *chain* of decays: B can decay into products, which are themselves unstable, and so on. An example is the decay of radon, a naturally occurring gas which can be found in basements of some buildings.

$$^{222}\mathrm{Rn} \rightarrow \alpha + ^{218}\mathrm{Po} \rightarrow \alpha + ^{214}Pb \rightarrow \ldots \tag{4.22}$$

which in turn is produced by decay of thorium, which is produced by Uranium decays:

$$^{230}\mathrm{Th} \rightarrow \alpha + ^{226}\mathrm{Ra} \rightarrow \alpha + ^{222}\mathrm{Rn} \tag{4.23}$$

For α decays, there are only 4 possible chains of nuclides (Table 4.3): those whose mass number A is exactly divisible by 4 ($A = 4n$) and those whose number of nucleons is $A = 4n + 1$ or $A = 4n + 24$, or $A = 4n + 3$, where n is a positive integer. The corresponding series are called: thorium series ($A = 4n$), neptunium series, uranium series (Fig. 4.7) and actinium series ($A = 4n + 3$). The Neptunium series ($A = 4n + 1$) contains no nuclide with extremely large lifetime. The majority of the radioactive elements of the neptunium series are already extinct since their formation in a supernova, about five billion years ago.

Table 4.3 Table of the four possible series of α decay chains

Series	A	Final
Thorium	$A = 4n$	^{208}Pb
Neptunium	$A = 4n + 1$	^{205}Tl
Uranium	$A = 4n + 2$	^{206}Pb
Actinium	$A = 4n + 3$	^{207}Pb

The decay chains stop when they reach a stable nuclide, an isotope of lead or thallium

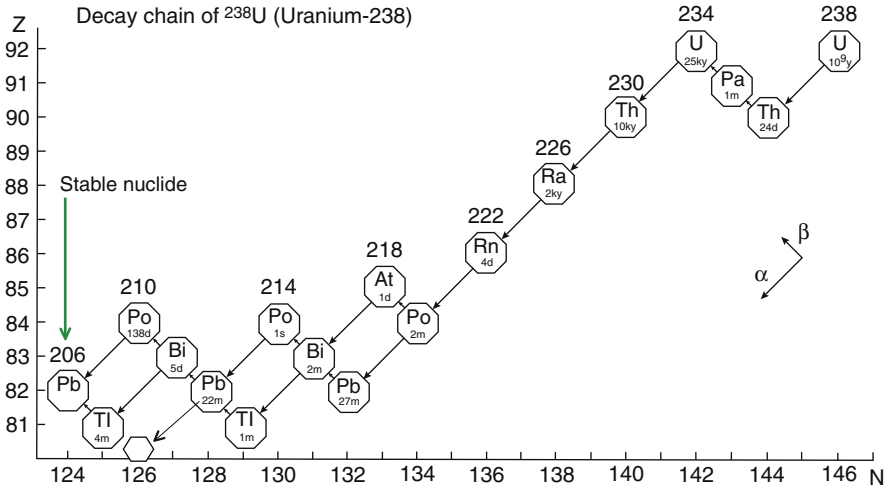

Fig. 4.7 The decay chain of ^{238}U is represented in the $N-Z$ plane. This representation of nuclides is called *Segrè chart*, from Emilio Segrè (1905–1989), who was awarded the Nobel prize in 1959 for the discovery of the anti-proton. N indicates the number of neutrons, $N + Z = A$. The α and β^- transitions are represented in an intuitive way. Figure from E. Segrè, "Nuclei and particles", W. Benjamin, Inc., 1965

Suppose to have the following reactions, where R_j indicates radioactive nuclides and $N_j(t)$ its corresponding number of nuclei present, or concentration at time t:

$$R_1 \rightarrow R_2 + A \tag{4.24}$$

$$R_2 \rightarrow R_3 + B \tag{4.25}$$

$$R_3 \rightarrow R_4 + C \tag{4.26}$$

The grand-parent radioactive nuclide R_1 follows a simple decay law $N_1 = N_1(0)e^{-\lambda_1 t}$, while the radioactive nuclide R_2 decays, but is also produced by the decay of R_1, so we can write

$$\frac{dN_2}{dt} = +\lambda_1 N_1 - \lambda_2 N_2 \tag{4.27}$$

and for nuclide R_3

$$\frac{dN_3}{dt} = +\lambda_2 N_2 - \lambda_3 N_3 \tag{4.28}$$

We have a chain of differential equations, which can be solved recursively. The general solution is reported below as a reference. It can be written in terms of sum of exponential decays, each term depends on the decay rate of all nuclides "above" in its genealogy tree.

$$N_1(t) = a_{11} e^{-\lambda_1 t} \tag{4.29}$$

$$N_2(t) = a_{21} e^{-\lambda_1 t} + a_{22} e^{-\lambda_2 t} \tag{4.30}$$

$$N_3(t) = a_{31} e^{-\lambda_1 t} + a_{32} e^{-\lambda_2 t} + a_{33} e^{-\lambda_3 t} \tag{4.31}$$

$$\dots \tag{4.32}$$

$$N_k(t) = a_{k1} e^{-\lambda_1 t} + a_{k2} e^{-\lambda_2 t} + \dots + a_{kk} e^{-\lambda_k t} \tag{4.33}$$

The coefficients a_{kj} with $k \neq j$ can be determined recursively:

$$a_{k,j} = a_{k-1,j} \frac{\lambda_{k-1}}{\lambda_k - \lambda_j} \tag{4.34}$$

and the "diagonal" coefficients must be determined by the initial conditions $N_k(0)$:

$$N_k(0) = a_{k1} + a_{k2} + \dots + a_{kk} \tag{4.35}$$

A notable case is when only the radionuclide R_1 is initially present: $N_k(0) = 0$ for $k > 1$:

$$N_1(t) = N_1(0) e^{-\lambda_1 t} \tag{4.36}$$

$$N_2(t) = N_1(0) \frac{\lambda_1}{\lambda_2 - \lambda_1} (e^{-\lambda_1 t} - e^{-\lambda_2 t}) \tag{4.37}$$

$$N_3(t) = N_1(0) \lambda_1 \lambda_2 \left(\frac{e^{-\lambda_1 t}}{(\lambda_2 - \lambda_1)(\lambda_2 - \lambda_1)} + \frac{e^{-\lambda_2 t}}{(\lambda_3 - \lambda_2)(\lambda_1 - \lambda_2)} + \frac{e^{-\lambda_3 t}}{(\lambda_1 - \lambda_3)(\lambda_2 - \lambda_3)} \right) \tag{4.38}$$

If, at a certain point of the decay chain, one nuclide, say R_s, has a lifetime much larger than the others (Figs. 4.8 and 4.9), we can have a notable case of equilibrium, which is called *transient equilibrium*, and it occurs when all "younger generations" decay with substantially the same decay constant as the nuclide with long lifetime R_s above them in the chain. The term *"secular equilibrium"* indicates that, in addition, we observe the decay on a timescale where we can approximate

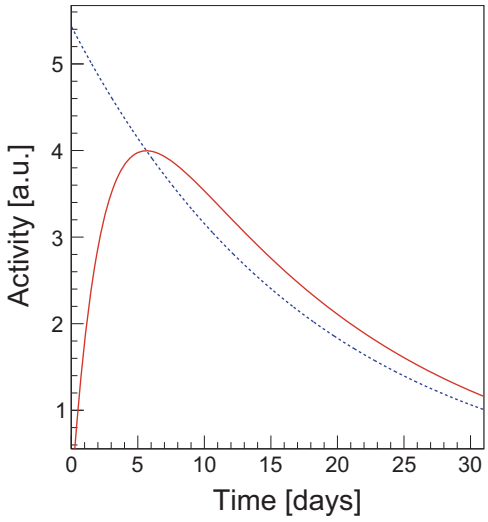

Fig. 4.8 An example of transient equilibrium, as it shows in the activity of a sample, which is initially composed of 100% Ba. The decay chain is: ^{140}Ba $\rightarrow ^{140}$ La $\rightarrow ^{140}$ Ce. The activity due to the parent is shown with a dashed line, and the activity of the daughter is represented by a solid line. The daughter nuclide ^{140}La has a lifetime 8 times smaller than the parent ^{140}Ba, and after a maximum the two curves follow each other. The activity of the daughter nuclide is larger than the activity of the parent

$e^{-\lambda_s t} = 1$. In this case for any R_t with $t > s$, we have

$$\frac{N_t}{N_s} = \frac{\lambda_s}{\lambda_t} \tag{4.39}$$

Uranium ores, for instance, are in secular equilibrium.

Another important case is when a nuclide is continuously formed, not by decay but with a nuclear reaction. Examples of such cases are the formation ^{14}C in the atmosphere and the activation of material in a particle accelerator. The differential equation is

$$\frac{dN}{dt} = Q - \lambda N(t) \ . \tag{4.40}$$

When the initial state is $N(0) = 0$, we have this solution:

$$N(t) = \frac{Q}{\lambda}(1 - e^{-\lambda t}) \ . \tag{4.41}$$

The nuclide ^{14}C is continuously produced in the atmosphere by cosmic rays, with a reaction reported in Eq. (7.36). We can consider the concentration of ^{14}C in the

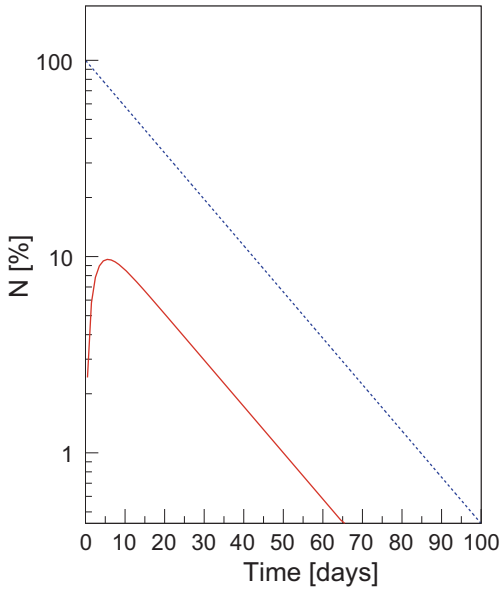

Fig. 4.9 The same decay as in Fig. 4.8 $^{140}\text{Ba} \rightarrow ^{140}\text{La} \rightarrow ^{140}\text{Ce}$ is used to illustrate the transient equilibrium, as in Eqs. (4.36) and (4.37). The fraction number of nuclides $N(t)/N_0(\text{Ba})$ existing at time t for Ba (dashed line) and La (solid line) is plotted as a function of time. After a transient, the two curves are almost parallel

atmospheric CO_2 to be constant in time: Eq. (4.41) for $t \rightarrow \infty$ gives $N(t) = Q/\lambda$. Corrections to the above equilibrium are due to human activities, like the 2055 nuclear explosions, which have increased the ^{14}C concentration; a peak of about twice the original value was reached in the mid of 1960s. Also, nuclear plants produce a negligible amount of ^{14}C, according to the reaction in Eq. (7.35). The use of fossil fuels, which are naturally depleted of ^{14}C by decay, dilutes its concentration in the atmosphere. The nuclear-test peak of $[^{14}C]$ concentration in air has an exponential decay, with a mean lifetime of about 23 years, which is much shorter than the decay time. This is due to its gradual absorption, mainly by vegetation. The present concentration level is about the same as before the nuclear tests.

4.4 Age Determination with Radioactive Nuclides

When living organisms die, they stop exchanging CO_2 with the atmosphere. If we assume that ^{14}C concentration was constant in the past, knowing the decay time of ^{14}C and measuring the concentration of ^{14}C in the sample, we can measure the time since the sample has stopped exchanging carbon with the atmosphere (Fig. 4.10). We can solve the simple decay formula for the time interval Δt:

$$\Delta t = -\tau \ln \frac{N(t)}{N_0} = \tau \ln \frac{N_0}{N_{\text{sample}}} , \tag{4.42}$$

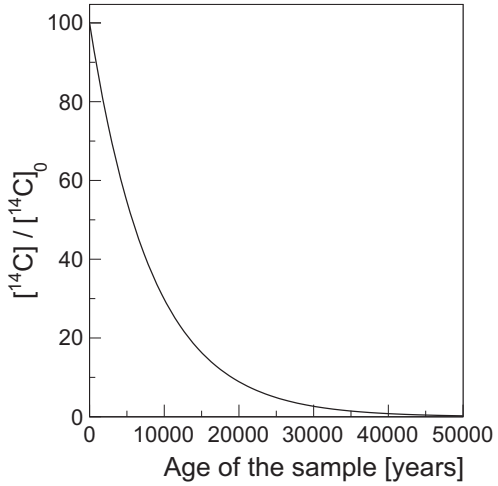

Fig. 4.10 Decay curve of ^{14}C, which is used for dating organic material. We measure the fraction of the radionuclide concentration with respect to the stable isotope [^{14}C]/[^{12}C] in the sample. We then divide this value by the same fraction, measured in present living material, or by the reference value. This value is reported on the y-axis, as a function of time before present. This method was invented and published in 1946 by Willard F. Libby (1908–1980), from the USA, who taught at the University of Chicago and was awarded the Nobel prize in chemistry in 1960

where N_0 in this case is the concentration of ^{14}C in a sample exchanging CO_2 and $N(t)$ is the concentration of ^{14}C in our "historical" sample. ^{14}C decays β^- with a mean lifetime of 8267 years and an end-point energy of 156 keV. Precise dating with radiocarbon is sensitive to the natural variations of ^{14}C concentration in the atmosphere. Because of the peak due to nuclear tests, the standard concentration of ^{14}C is assumed as the value measured in 1950 and corresponds to a concentration of 1.30×10^{-12} with respect to all atoms of carbon. Radiocarbon dating is calibrated with increasing precision using information from tree rings and from analysing the air samples trapped in the ice layers in Greenland and Antarctica. Recent studies suggest that a considerable modulation in ^{14}C concentration occurred in a time interval of 30,000–45,000 years ago.

Other nuclides are used for longer time constants. In particular, the ratio between the concentrations of parent and daughter nuclides gives information on the time when a particular rock became solid. The principle is that since the solidification occurred, the daughter atoms stayed in place in the sample. The potassium–argon method uses ^{40}K, which has a half-life of 1.28×10^9 years; this is about 1.3 billion years, to be compared to the age of the Earth, which is 4.54 billion years. Therefore, this nuclide is useful for geological dating. It decays by *electron capture* to ^{40}Ar, which is chemically inert and escapes from the fluid magma, but remains trapped in solid rock.

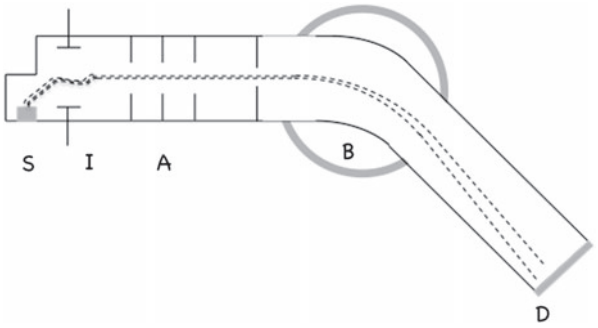

Fig. 4.11 Sketch of a mass spectrometer: (S) Sample, which is vaporised in vacuum, (I) ionisation, (A) accelerator, (B) magnetic field perpendicular to the drawing and (D) detector

4.5 Technical Aspects: The Mass Spectrometer

It would be intuitive to measure the concentration of a radionuclide for age determination by measuring the activity of the sample. However, a simple calculation reveals that in most cases it is impractical or impossible to detect this radiation. A very powerful tool comes to our help: the *mass spectrometer* (Fig. 4.11). The sample is first pulverised, or purified with chemical methods. When heated in vacuum, its vaporised atoms are first ionised, then accelerated. The ion beam traverses an area with a magnetic field, and ions are deflected differently according to their different mass over charge ratio m/q. A detector at the end of the vacuum pipe is spatially segmented, to count the signals from single ions in different positions corresponding to different m/q values. This method allows us to measure the relative abundance of isotopes of the same chemical element present in the sample. It is also clear that this technique of dating with radioactive nuclides is destructive for the sample. It is clear that both the precision and the maximum age determination depend on the weight of the sample and on its chemical composition. Modern radiocarbon techniques can reach dating up to 70,000 years ago, while other nuclides are used for dating older samples.

4.6 Radioactive Iodine for Thyroid Cancer

This is a case study, to attract the reader's interest to a practical case. The numerical values used are representative of a real case, although in practice there are many other factors to be considered.

Thyroid cancer is cured with radioactive iodine-131, which accumulates in the thyroid much more than in other organs. The nuclide ^{131}I decays β^-, with an end-point electron energy of 606 keV. These β^- particles ionize the fluid, and the resulting ions damage the surrounding cancer cells. The daughter nuclide is formed

in an excited state and emits a γ ray of energy $E_\gamma = 364\,\text{keV}$. The atomic weight of iodine is $A = 131$ and its half-life is 8.02 days.

1. What particles and nuclides are produced in this decay? (use the periodic table)
2. How many grams of iodine are needed to prepare a drink with initial activity 1.85 GBq? What would you use to precisely measure this quantity?
3. What would block this β radiation?
4. What type of radiation can be detected outside the patient's body?
5. Neglecting any disposal of iodine, how long the patient must be in isolation to see its thyroid radioactivity decreased to an acceptable level of 500 Bq?
6. 90% of the iodine is eliminated by the body in 3 days. Compare this time with the decay time above, and suggest the appropriate measures to the hospital.

Discussion

1. *What particles and nuclides are produced in the β^- decay of ^{131}I?*

   The β^- decay produces an electron with a continuum spectrum (as opposed to a single spectral line of monoenergetic particles). To conserve energy, another neutral particle, which escapes detection, must be emitted. This is the electron anti-neutrino $\overline{\nu_e}$. A neutron in the nucleus becomes a proton, thus the nuclide keeps the same mass number A and adds one to its atomic number, moving by one place to the right in the periodic table. To the right of iodine, we find Xenon, so the reaction is

$$^{131}I \rightarrow ^{131}\text{Xe} + e^- + \overline{\nu}_e$$

2. *How many grams of ^{131}I are needed to prepare a drink with initial activity 1.8 GBq?*

$$t_{1/2}(^{131}\text{I}) = 8.82\,\text{days} = 8.02 \times 24 \times 3600 = 6.93 \times 10^5\text{s}.$$

$$\tau = t_{1/2}/\ln 2 \approx 1.44 \times t_{1/2} = 9.95 \times 10^5\ \text{s}$$

$$\text{activity } A = \lambda N(t) = \frac{N(t)}{\tau} = \frac{N_0 e^{-\frac{t}{\tau}}}{\tau}$$

We are interested to the number of nuclei for a given initial activity, i.e. at $t = 0$.

$$N_0 = \tau A = 9.98 \times 10^5 \times 1.8 \times 10^9 = 1.8 \times 10^{14}$$

We know that 6.022×10^{23} atoms (Avogadro's number) have a mass of A (mass number) grams. Therefore, in terms of mass: 1.8×10^{14} atoms of Iodine have a mass w:

$$w = \frac{1.8 \times 10^{14}}{6.022 \times 10^{23}} \times 131\ \text{g} = 39.1 \times 10^{-9}\ \text{g} = 39.1\ \text{ng}$$

Modern analytical balances typically need samples of 1 mg or more, and have a sensitivity of about 100 ng. To measure this small quantity of 40 ng, we cannot use a balance; the mass is measured indirectly by measuring the activity, with using a radiation detector and a rate metre.

3. *What would block this β radiation?*
   The β radiation of iodine-131 has an end-point of 606 keV and is blocked by a few millimetres of living tissue, which is mostly water. Incidentally, this is the very reason why this kind of radiation destroys cancer cells: beta radiation delivers energy to the cancer cells or to their surrounding fluid and the resulting ions damage the cells. The thyroid is under a few millimetres of neck skin.

   As a result, the beta radiation is blocked primarily by the cancer cells and by the surrounding tissue. The range of 606 keV beta particles in air is of the order of 30–50 cm.
4. *What type of radiation can be detected outside the patient's body?*
   To a first approximation, only the γ radiation emitted by the daughter nucleus can be detected from outside the patient body. What follows is a more detailed explanation. The xenon nucleus, which is formed by the beta decay of the Iodine, finds itself surrounded by the electron cloud of the iodine, which has one electron less. An electron fills the lowest energy level of Xe, which is lower than the corresponding lowest level of Iodine. The atom emits X-rays with energies up to the κ_β energy of Xe, which is 33.6 keV. The γ radiation from the electromagnetic decay of the excited Xe nucleus has an energy of 364 keV. The passage of X-rays through the matter will be introduced in the next chapter. An important parameter for calculating the attenuation at low energies is the highest X-ray energy which can be emitted by the atom. This value is normally referred to as the k_α and κ_β spectral lines (Fig. 4.12). The energy values of both the X and the γ ray are above any k_α line of light elements which make living tissue. As a comparison, the k_α line of Calcium in the bones is at 3.7 keV. Therefore, the gamma ray attenuation in the body is very small. Most of the γ and X radiation escapes the patient body and can be detected outside. For each β^- particle emitted by the Iodine-131, there is a γ ray of a specific energy emitted by the Xe nucleus and an X-ray emitted by the Xe atom. By measuring the γ activity outside the patient body, we also measure the β activity of the administered dose. The X-ray activity for one particular energy transition can be calculated with atomic transition probabilities and *selection rules* and its calculation is outside the scope of this book.
5. *How long the patient must be in isolation to see its activity to decay to* 500 *Bq, neglecting any disposal by fluid exchanges?*

$$A(t) = (1/\tau)N(t) = (1/\tau)N_0 e^{-\frac{t}{\tau}} = A_0 e^{-\frac{t}{\tau}}$$

$$\frac{A(t)}{A_0} = e^{-\frac{t}{\tau}}$$

$$t = \tau \ln \frac{A_0}{A(t)} = 9.95 \times 10^5 \times \ln \frac{1.8 \times 10^9}{500} = 15.2 \times 10^6 \text{ s} = 174 \text{ days}$$

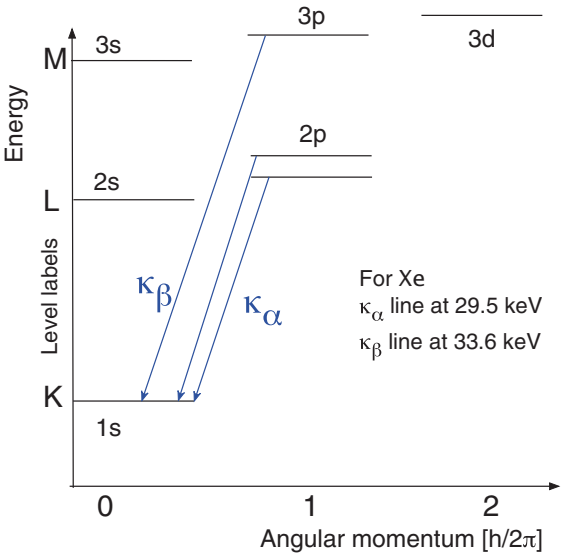

Fig. 4.12 The most intense sources of X-rays are atomic transitions to the lowest electron energy level. The energy levels are named as K, L, M or $1, 2, 3,$ according to the main energy level and "s, p, d" are states of angular momentum 0, 1, 2, respectively. Transitions from states, or *orbitals* $2p$ to $1s$, originate what are called k_α spectral lines, which are typically in the X-ray range. Transitions from $3p$ to $1s$ originate the k_β lines, which have higher energy than the k_α lines, but often have a lower intensity

6. 90% *of the iodine is eliminated by the body in* 3 *days. Compare this time with the decay time above and suggest the appropriate measures to the hospital.* In reality, patients have to stay in isolation only a few days, because iodine is eliminated by the body much faster. However, patient's fluids have to be considered as radioactive waste for a few months.

4.7 Problems

4.1 One of the products of the decay chain of ^{241}Am is ^{213}Bi (Bismuth), which undergoes both α and β decay (see text). We have to measure the activity of a sample of pure ^{213}Bi. Our particle detector is wrapped in a thin aluminium foil and is only sensitive to beta particles, with an efficiency of 80%; our experimental set-up has a geometrical acceptance of 50%. At a given time, we measure a counting rate of 100 Hz. What is the total activity of the source? We measure the activity for 20 s, at regular intervals of 10 min, we plot the data, and we fit with an exponential curve, obtaining a mean decay time of 45.6 min. Is any correction needed to this measurement due to the fact that we only observe one decay mode? What value of the lifetime would we have measured if the detector were sensitive to α particles only?

4.2 Radioactive humans: an average human body of 70 kg contains 18% of carbon. With the data present in the text, calculate the "human activity" due to ^{14}C.

4.3 The material from a corner of a papyrus is analysed with mass spectrometer techniques. The ratio $[^{14}\mathrm{C}]/[^{12}\mathrm{C}] = 0.79 \times 10^{-12}$. What is the age of the papyrus?

4.4 Some alcohol from a wine bottle is extracted and analysed with a mass spectrometer, showing a ratio $[^{14}\mathrm{C}]/[^{12}\mathrm{C}] = 1.95 \times 10^{-12}$. Explain the anomaly and give an approximate age of the bottle, using the data which is given in the text.

4.5 A parent nucleus decays with probability λ_1 per unit time. Its daughter decays with probability λ_2 per unit time. Starting from a pure sample of the parent, show that the time at which the number of daughter nuclei is a maximum:

$$t_{\max} = \frac{1}{\lambda_2 - \lambda_1} \ln\left(\frac{\lambda_2}{\lambda_1}\right).$$

4.8 Solutions

Solution to 4.1 The total activity includes all decays, in this case both α and β, and is counted over the whole solid angle. Therefore, we have to correct by the detector efficiency and by the solid angle *acceptance* and by the branching fraction:

$$A = \frac{\text{rate}}{\text{acceptance} \times \text{efficiency} \times \text{BR}} = \frac{100}{0.978 \times 0.8 \times 0.5} = 255.6\ \text{Bq}$$

In general, efficiency and acceptance have an experimental systematic error, which is added to the statistical error of the counting rate. No correction is needed to the measurement: the lifetime is a characteristic of the nuclide. When measuring the lifetime with a detector which is sensitive only to α particles, we would observe exactly the same value.

Solution to 4.2 The amount of carbon in a 67-kg human body is 12.05 kg, which is about 10^3 moles. We know that the concentration of $[^{14}\mathrm{C}] = 1.30 \times 10^{-12}$, so the number of atoms of radiocarbon is

$$N_{14} = 10^3 \times N_A \times \left[^{14}\mathrm{C}\right] = 10^3 \times 6.02 \times 10^{23} \times 1.30 \times 10^{-12} = 7.82 \times 10^{14}$$

Now, the average lifetime is

$$\tau = 8627\ \text{years} \times 31.536 \times 10^6\ \text{s/year} = 2.721 \times 10^{11}\ \text{s}$$

The activity is

$$A = 1/\tau N_{14} = \frac{7.82 \times 10^{14}}{2.721 \times 10^{11}} = 2.87 \times 10^3\ \text{Bq} = 2.87\ \text{kBq}$$

In addition to a constant bombardment by cosmic rays, the human body is subject to radiation from inside. Also, radioactive K is a source of radiation.

Solution to 4.3 From Eq. (4.42):

$$\Delta t = -\tau \ln \frac{N(t)}{N_0} = -8627 \text{ years } \ln \frac{0.79 \times 10^{-12}}{1.30 \times 10^{-12}} = 4300 \text{ years before present}$$

The papyrus can be dated to 2300 BC.

Solution to 4.4 The radiocarbon concentration of the sample has a value $[^{14}C]/[^{12}C] = 1.95 \times 10^{-12}$, which is higher than the standard concentration, 1.30×10^{-12}. This means that the sample can be dated in a period during the so-called bomb-peak of ^{14}C. Neglecting the radioactive decay, which has a lifetime of 8627 years, we can use the exponential decay of the *excess* of radiocarbon, which has a lifetime $\tau = 23$ years, to find the year when the radiocarbon concentration was the same as the one found in the sample. We can use the same formulas, but for the excess of $[^{14}C]$, which reached its maximum value of twice the normal value in 1965.

$$N(t) - N_0 = (N_{\max} - N_0)e^{-\Delta t/\tau} \Rightarrow \Delta t = -\tau \ln((N(t) - N_0)/N_0) =$$

$$= 23 \times \ln((1.95 - 1.30)/1.30) = 16 \text{ years after the peak } \approx 1981$$

Solution to 4.5 The problem is simply solved by finding the maximum of the function in Eq. (4.36):

$$N_2(t) = N_1(0) \frac{\lambda_1}{\lambda_2 - \lambda_1} \left(e^{-\lambda_1 t} - e^{-\lambda_2 t}\right)$$

$$\frac{dN_2}{dt} = 0 = \frac{\lambda_1}{\lambda_2 - \lambda_1} \left(-\lambda_1 e^{-\lambda_1 t} + \lambda_2 e^{-\lambda_2 t}\right)$$

for $\lambda_1 \neq 0$

$$\lambda_1 e^{-\lambda_1 t} = \lambda_2 e^{-\lambda_2 t} \text{ and taking logs on both sides:}$$

$$-\lambda_1 t = \ln \frac{\lambda_2}{\lambda_1} (-\lambda_2 t)$$

$$(\lambda_1 - \lambda_2)\, t_{\max} = \ln \left(\frac{\lambda_2}{\lambda_1}\right)$$

Bibliography and Further Reading

H.D. Graven, Impact of fossil fuel emissions on atmospheric radiocarbon and various applications of radiocarbon over this century. Proc. Natl. Acad. Sci. USA **112**(31), 9542–9545 (2015)
B.R. Martin, *Nuclear and Particle Physics: An Introduction* (Wiley, Chichester, 2011)
E. Segré, *Nuclear and Particle Physics* (W. A. Benjamin, Reading, 1977)

Chapter 5
Passage of Radiation Through Matter

5.1 Introduction

In this chapter a more practical aspect of radiation is described: its interaction with matter. It has importance both for shielding and for detecting radiation. We'll limit the scope to X and γ rays for the electromagnetic radiation, to charged particles like α, $\beta^{\pm}$ and cosmic rays and, very schematically to *neutrinos*, leaving neutron interactions to the nuclear physics chapter.

Radiation interacts with matter by means of *scattering* processes: the initial radiation can be absorbed, deviated or can be transmitted (Fig. 5.1). In the first case all the initial energy is released in the medium, in the second case only a fraction of it. Initially we'll consider the common aspects of scattering, then the peculiarities of each type of radiation will be described. In the initial sections we focus on what happens to the radiation, while the effects on the material will be covered in the last two sections of this chapter: radiation detectors and biological effects.

5.2 The Effective Cross Section

We consider the case where we have a flux of incident radiation, which is measured in terms of number N_i of *i*ncident *photons* or charged particles per unit surface per second:

$$J = \frac{N_i}{S\,t}\ , \tag{5.1}$$

where S is the surface and t the time duration of the process. We assume that within that surface S the density is constant, or in other words J is constant in the considered time interval. We define the *intensity* I as the number of incident

S. D'Auria, *Introduction to Nuclear and Particle Physics*,
Undergraduate Lecture Notes in Physics,
https://doi.org/10.1007/978-3-319-93855-4_5

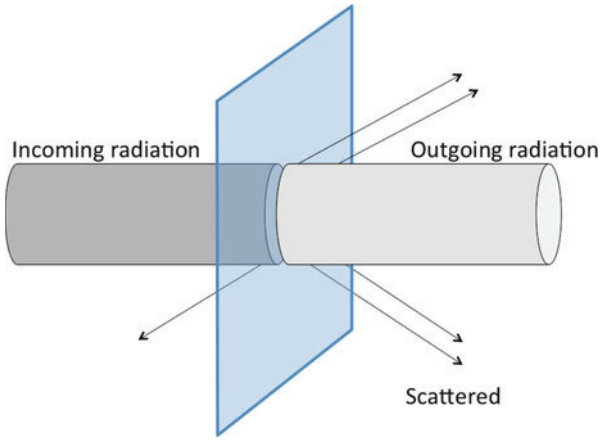

Fig. 5.1 Schematics of passage of radiation through a thin layer of material. Part of the radiation is transmitted, part is scattered or absorbed

particles per unit of time:

$$I = \frac{N_i}{t} \; ; \tag{5.2}$$

In case the incoming radiation beam is not uniformly distributed, the intensity is the integral of the flux over the surface:

$$I = \int_S J(x, y) dx \, dy \tag{5.3}$$

The material is characterised by its density and by its chemical composition. It is reasonable to expect that a layer of liquid nitrogen absorbs more radiation than a layer of air, which is mostly nitrogen, of the same thickness, just because there are more scattering centres per unit of volume. Each scattering centre can be more or less efficient in scattering, depending on its apparent "size". This is parametrised by another quantity, which depends both on the impinging radiation and on the material: it is the *effective cross* section, it is indicated with σ and is a characteristic property of all scattering processes. It depends on the nature and kinetic energy of the incoming particle, on the process that takes place and, of course, on the material composition. The concept of cross section can be extended to other situations, like colliding particle beams. From a qualitative point of view it is reasonable to expect that a radiation with a small wavelength or high energy (Eq. (3.3)) is less attenuated than a radiation with larger wavelength, for a given material. For a given wavelength it is reasonable to expect that atoms with larger numbers of electrons each have a larger probability to interact with radiation compared with a material with lower Z. The term *cross section* derives from experiments on fixed targets, like the scattering of α particles on a gold foil, as first done by E. Rutherford, H. Geiger and E. Marsden

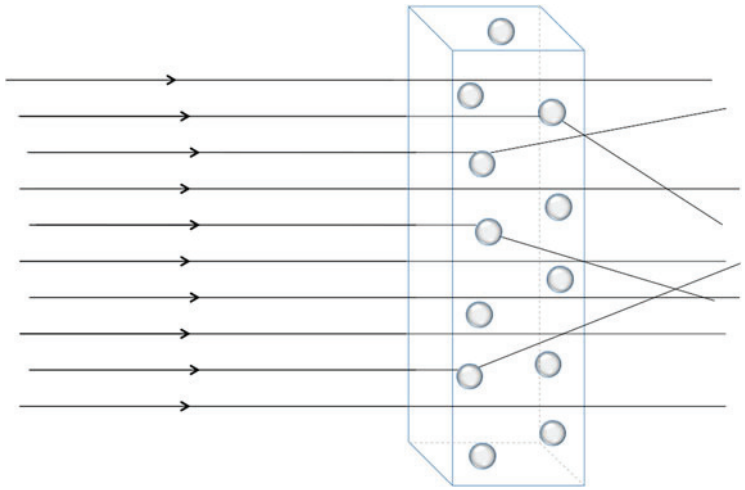

Fig. 5.2 Scattering of particles from a target. The scattering probability is larger for a larger density of the target and depends on the quantum probability of interacting with a single scattering centre. This quantity is the *cross section* σ, the apparent size of a scattering centre, which depends on the type and energy of the incident radiation. Figure adapted from Povh et al. (2015)

Ernest Rutherford (1871–1937) from New Zealand was awarded the Nobel prize in chemistry in 1908 for having demonstrated that radioactive decays induce a transmutation of elements, but he is most famous for the experiment that demonstrated that majority of atomic mass is concentrated in the nucleus.

in 1909, which demonstrated the existence of a relatively massive nucleus inside Au atoms. The radiation may interact with atoms, single electrons or nuclei in the target, which appear to have an *effective* size, which changes as a function of the energy and the type of the incoming particle. The probability of hitting a target is proportional to the target area perpendicular to the direction of the projectiles, as sketched in Fig. 5.2. When there are many targets, the probability also depends on their density, in terms of targets per unit of surface. In general, we know the density ρ of a material in terms of kg/m^3 or g/cm^3; we obtain the *atomic density* $\mathcal{N}$ by dividing ρ by the mass of a single atom. Equivalently, if M indicates the atomic mass of the material, which we assume is made by a pure element, like gold or lead, and N_A represents Avogadro's number,

$$\mathcal{N} = \frac{\rho\, N_A}{M} \tag{5.4}$$

The number of scattering centres "seen" by an incoming particle depends on this density and on the thickness δx of the absorber. In the following we assume that the thickness is small so that we have no shadowing effect, and that the material is not a

crystal, so that there is no special direction of propagation. The number of scattered or absorbed particles, N_s, is proportional to the number of incident particles N_i, to the cross section $\sigma_p(E)$ for that particular process and for that particular energy range, to the density of scattering centres and to the thickness of the target:

$$N_s = N_i \frac{\rho\, N_A}{M}\, \delta x\, \sigma_p(E) \quad \text{and} \quad R_s = I_i\, \frac{\rho\, N_A}{M}\, \delta x\, \sigma_p(E)\ , \tag{5.5}$$

where the scattering rate R_s is the number of scattering interactions per unit of time and I_i is the incident intensity.

Conversely, we can read from the formulas above that the effective cross section of a scattering process is the number of interactions per unit time per target particle per unit of incident flux. So, the effective cross section is the expression of the quantum-mechanical probability that a scattering occurs. As the scattering process is the same for any boost along the direction of the incoming particles, its description is relativistically invariant.

Given a type of radiation and a material, more than one process may be possible. In this case, the total cross section is the sum of the cross sections of the single processes. As an example, looking at Fig. 5.6, for photons of 1.5 MeV all three processes are possible: Compton scattering, photoelectric effect and pair creation. The total cross section, which we use to calculate the attenuation coefficient of the radiation, is the sum of these three cross sections:

$$\sigma_{\text{tot}} = Z\sigma_C + \sigma_{\text{pe}} + \sigma_{ee} \tag{5.6}$$

If the target material is a chemical compound or a mixture, the individual scattering rates of each element are added.

The total cross section has physical dimensions of $[L^2]$; in nuclear and particle physics the unit is the *barn*:

$$1\ \text{barn} = 10^{-28}\ \text{m}^2 = 100\ \text{fm}^2 \tag{5.7}$$

and its sub-multiples millibarn (mb), nanobarn (nb), picobarn (pb) and femtobarn (fb).

For a given scattering process it may be relevant to calculate also the probability that the scattering occurs to a particular final state, e.g. the probability (or rate) to scatter a photon to a given solid angle interval around a direction, or in a given energy or momentum interval. The formulas are the same as in Eq. (5.5) but we use the *differential cross section*, which are indicated as (Fig. 5.3):

$$\frac{d\sigma}{d\Omega}; \quad \frac{d\sigma}{dp}; \quad \frac{d\sigma}{dE} \tag{5.8}$$

for solid angle, momentum and energy, respectively. These distribution functions give the scattering probability to a given interval of final states. Double differential

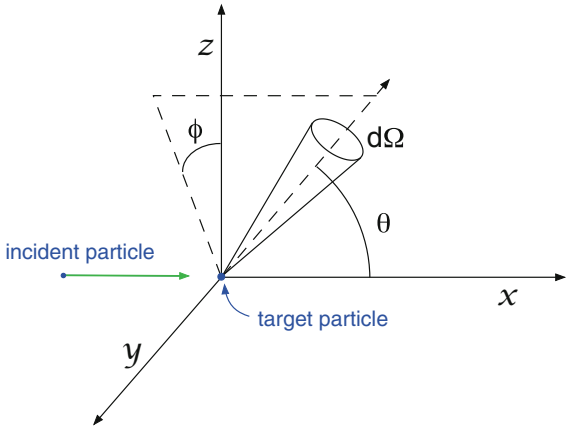

Fig. 5.3 dΩ is the solid angle. The total cross section for a process is proportional to the interaction probability. The differential cross section $d\sigma/d\Omega$ gives the probability that a given outgoing particle is scattered at a certain solid angle. Another example is $d\sigma/dE$ for the probability of an outgoing particle to have an energy between E and $E + dE$

cross sections are two-dimensional distributions of scattering probability:

$$\frac{d^2\sigma}{d\Omega\, dp} \tag{5.9}$$

Integrating over the whole solid angle and over the momentum, we recover the cross section.

5.3 Scattering of Electromagnetic Radiation

Electromagnetic waves with short wavelength, like X- and γ-rays, interact with matter in four principal processes:

- Rayleigh scattering occurs when light interacts with an atom and is scattered at a different angle, without ionising or exciting it.
- The photoelectric effect occurs when light interacts with an atom and expels an electron (Fig. 5.4).
- Compton scattering occurs when a photon interacts with a single electron of an atom (Fig. 5.5).
- The photon can "split" into an electron and positron pair if it has enough energy and interacts with the electric field of a nucleus. This process is called *electron–positron pair creation*.

For a given photon energy, each of the processes above has a different probability of occurring. The probability of each process depends on the photon energy in a different way. The total *cross section* is the sum of the cross section, or Q-M. probability, of each process, as shown in Fig. 5.6. In the Rayleigh scattering process the electromagnetic radiation interacts with the atom or molecule as a whole and is just deviated, not absorbed. For a given atom or molecule, the cross section varies with the wavelength as $1/\lambda^4$, it is larger for short wavelength, like those corresponding to the blue colour; this qualitatively explains the blue colour of the sky.

Fig. 5.4 Photoelectric effect. Note that the photon is absorbed by the atom, which expels an electron

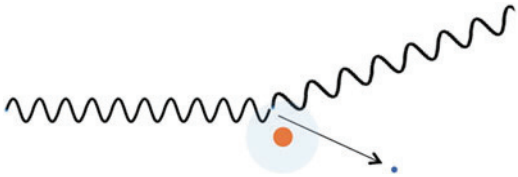

Fig. 5.5 Compton scattering. The photon interacts with the electron, transferring momentum. The electron is emitted and also a photon is emitted at an angle with respect to the impinging photon

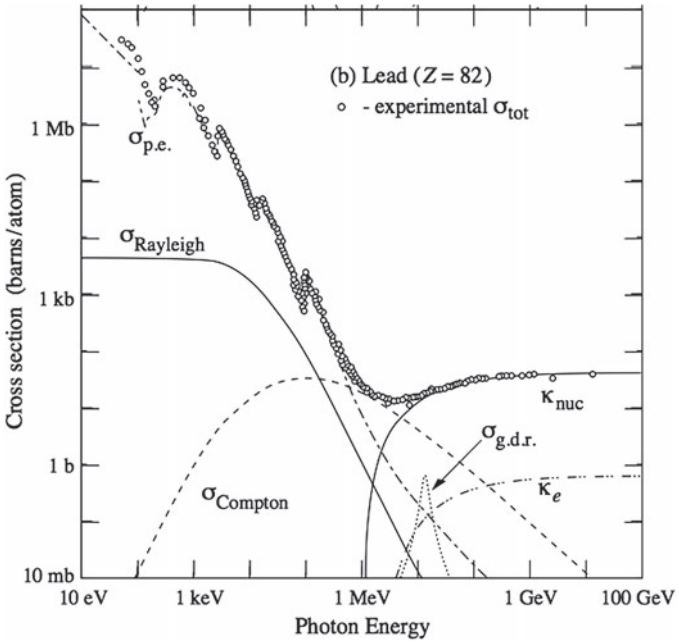

Fig. 5.6 Cross section of lead atoms Pb, as "seen" by photons in a large energy range. The calculated cross sections of single processes are also shown. The absorption and scattering of photons in the matter is the sum of several fundamental processes. Reprinted with permission from M. Tanabashi et al. (Review of Particle Physics), Phys. Rev. D, vol. 98-1, p. 454 (2018). Copyright (2018) by the American Physical Society. The unit used in the cross section is the *barn*, (b), defined as $1\ \mathrm{b} = 100\ \mathrm{fm}^2 = 10^{-28}\ \mathrm{m}^2$

5.4 Attenuation of Electromagnetic Radiation

If the energy of the light is larger than the minimum ionisation energy of the target atoms the *photoelectric effect* may occur. In this case the atom absorbs a photon and expels an electron. With higher photon energies electrons from inner shells can be excited. Qualitatively, inner electron shells are also closer to the nucleus, making a smaller target for the photon; also the wavelength of the photon is smaller, so both effects contribute to a decrease of the cross section when increasing the photon energy.

The practical limits in terms of photon energy for the photoelectric effect to occur for a given element are given by the lowest ionisation energy and by the energy corresponding to the k_β X-ray emission line of the atom, which is close to the maximum energy transition in an atom, as shown in Fig. 4.12. For photon energies above the *K-edge* the photoelectric effect still occurs, but at a lower rate.

The photoelectric process completely removes photons from the initial beam. Starting from Eq. (5.5), the scattering rate R_s is the amount of intensity removed from the beam:

$$R_s = I_{\text{incident}} - I_{\text{transmitted}} = -\delta I \ = \rho\sigma \frac{N_A}{M} I_i \, \delta x \ . \tag{5.10}$$

Using

$$\mu = \rho \frac{N_A}{M} \sigma \ = \mathcal{N}\sigma \ \text{ we have: } \delta I = -\mu \, I_i \, \delta x; \quad \frac{\delta I}{\delta x} = -I_0 \, \mu \tag{5.11}$$

Replacing small quantities with infinitesimal quantities, we have a differential equation

$$\frac{dI(x)}{dx} = -\mu \, I(x) \text{ , whose solution is: } \ I(x) = I_i \, e^{-\mu x} \tag{5.12}$$

This function is shown in Fig. 5.7. The parameter μ has physical dimensions $[L^{-1}]$ and is called the *attenuation coefficient*. It depends on the density of the absorber and on the cross section, which is a function of the energy of the radiation. In general a given material may have different densities, so the density is factored out in most tables and calculations which report μ/ρ in cm^2/g. This means that we need to multiply this value by the density of the material to obtain the value to use in Eq. (5.12).

The cross section for the photoelectric effect, in a given material, varies with the photon energy as

$$\sigma_{\text{p.e.}} \propto \frac{1}{E_\gamma^3} \tag{5.13}$$

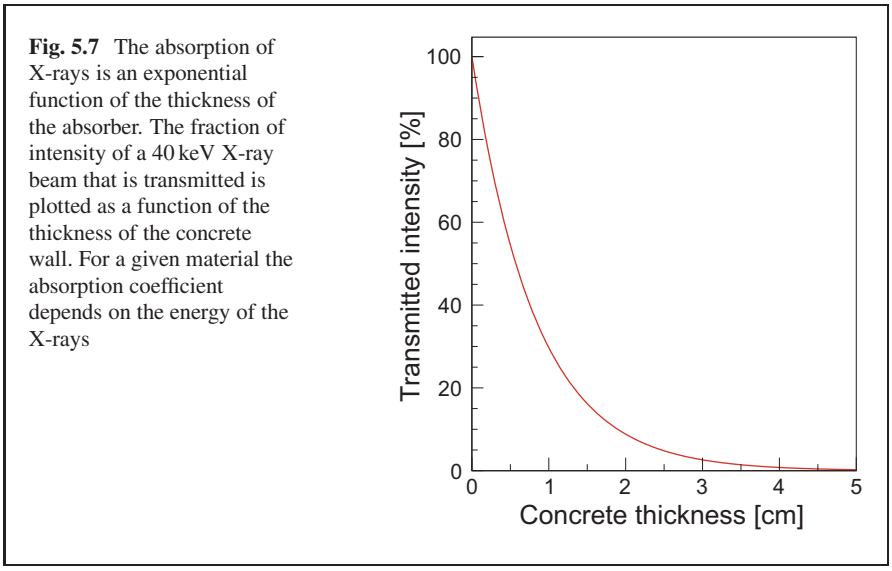

Fig. 5.7 The absorption of X-rays is an exponential function of the thickness of the absorber. The fraction of intensity of a 40 keV X-ray beam that is transmitted is plotted as a function of the thickness of the concrete wall. For a given material the absorption coefficient depends on the energy of the X-rays

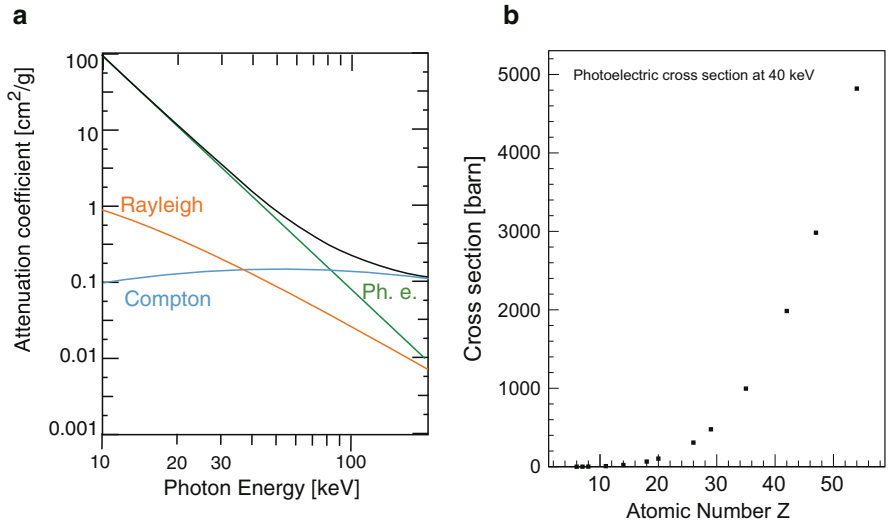

Fig. 5.8 (**a**) Left: attenuation coefficient of calcium as a function of the photon energy. The contributions from three processes (Rayleigh, Compton scattering and photoelectric) are shown separately, and as a sum.
(**b**) Right: cross section per atom for the photoelectric process for 40 keV X-ray photons, as a function of the atomic number of the absorber. The best fit to these data gives a power law with exponent 4.2 at this energy. Data from National Institute of Standards and Technology Standard Reference Data Program

but the curve presents several discontinuities at values corresponding to the energy levels of the atoms, as shown in Fig. 5.6. For a given photon energy, the photoelectric cross section increases with the fourth power of the atomic number Z, as shown in Fig. 5.8b:

$$\sigma_{\text{p.e.}} \propto Z^n \ ; \ \text{with} \quad 4 \leq n \leq 4.6 \ , \quad \text{at fixed } E_\gamma \tag{5.14}$$

Below a threshold energy, which depends on the material, photons are unable to ionise and can only be diffused by the material. Above a material-dependent energy value, photons interact predominantly with electrons rather than with the atom as a whole.

5.5 Compton Scattering

Compton[1] scattering occurs when photons interact with single electrons in the cloud of an atom. The cross section is a function of the photon energy and increases linearly with the electron density, which is proportional to Z. From the practical point of view it becomes the dominant scattering mechanism for photons in an energy range around 0.1–1 MeV, the limits depending on the material Z.

The kinematics are simple: a massless particle hits a massive particle, an electron, which is considered to be at rest. With the help of special relativity we can calculate the energy of the scattered photon as a function of the scattering angle and of the initial photon energy.

For a particle with $m \neq 0$ and 4-momentum $\mathbf{p} = (\frac{\gamma mc^2}{c}, p_x, p_y, p_z)$ we calculate the invariant mass $\sqrt{\mathbf{pp}}$ in the reference frame where the particle is at rest and $\vec{p} = 0$ and $\gamma = 1$. As it is a 4-vector, this quantity, the invariant mass, remains invariant, and is $\sqrt{\mathbf{pp}} = mc$, or in a general form

$$\mathbf{pp} = \frac{E^2}{c^2} - p^2 = m^2c^2 \quad \text{or} \tag{5.15}$$

$$E^2 - p^2c^2 = m^2c^4 \tag{5.16}$$

It is invariant because if we consider the entire system, before and after a decay or any reaction, it does not change.

The scattering process we are going to describe is:

$$\gamma + e^- \rightarrow \gamma + e^- \tag{5.17}$$

We neglect the binding energy of the electron to the atom, because this is typically of the order of few eV, and solve the kinematic in the reference frame where

[1] After Arthur H. Compton (1892–1962) from USA. He was awarded the Nobel prize in 1927 "for the discovery of the effect named after him".

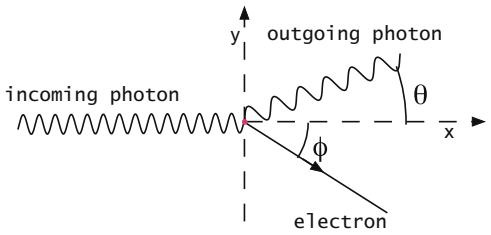

Fig. 5.9 Compton scattering

the electron is initially at rest. It is clear that the scattering process occurs in a geometrical plane containing the momenta of all particles involved. We assume this is the $x - y$ plane, and we neglect the z coordinate. In general, the incoming and outgoing photons will not have the same energy. Let E_0 be the energy of the incoming photon and E_1 the energy of the outgoing photon, as shown in Fig. 5.9. We apply momentum and energy conservation independently, and use the relativistic formulae:

$$p_x : \qquad E_0/c = (E_1/c)\cos\theta + p\cos\phi; \tag{5.18}$$

$$p_y : \qquad (E_1/c)\sin\theta - p\sin\phi = 0; \tag{5.19}$$

$$E : \qquad E_0 + mc^2 = E_1 + E_e \tag{5.20}$$

where $p = |\vec{p}|$ is the electron momentum, m is the electron mass and the angles ϕ and θ are measured between outgoing particles and the direction of the incoming photon. E_e is the electron energy.

From momentum conservation we have:

$$E_1 \sin\theta = pc\sin\phi; \tag{5.21}$$

$$E_0 - E_1\cos\theta = pc\cos\phi; \tag{5.22}$$

We square and sum:

$$E_1^2\sin^2\theta + (E_0 - E_1\cos\theta)^2 = p^2c^2(\sin^2\phi + \cos^2\phi); \tag{5.23}$$

$$E_1^2\sin^2\theta + E_0^2 + E_1^2\cos^2\theta - 2E_0E_1\cos\theta = p^2c^2; \tag{5.24}$$

$$E_1^2 + E_0^2 - 2E_0E_1\cos\theta = p^2c^2; \tag{5.25}$$

now $p^2c^2 = E_e^2 - m^2c^4$ from the electron 4-momentum. Using energy conservation we have

$$E_e^2 = ((E_0 - E_1) + mc^2)^2; \text{ subst. in 4-momentum} \tag{5.26}$$

$$p^2c^2 = (E_0 - E_1)^2 + m^2c^4 + 2mc^2(E_0 - E_1) - m^2c^4; \tag{5.27}$$

$$p^2c^2 = (E_0 - E_1)^2 + 2mc^2(E_0 - E_1) = E_0^2 + E_1^2 - 2E_0E_1\cos\theta; \tag{5.28}$$

$$E_0^2 + E_1^2 - 2E_0E_1 + 2mc^2(E_0 - E_1) = E_0^2 + E_1^2 - 2E_0E_1\cos\theta; \tag{5.29}$$

$$E_0 - E_1 = \frac{E_0E_1}{mc^2}(1 - \cos\theta) \tag{5.30}$$

Passing from energies to wavelengths: $E_j = h\nu_j = hc/\lambda_j$

$$E_0 - E_1 = hc\Big(\frac{1}{\lambda_0} - \frac{1}{\lambda_1}\Big) = hc\Big(\frac{\lambda_1 - \lambda_0}{\lambda_1\lambda_0}\Big) \tag{5.31}$$

$$\lambda_1 - \lambda_0 = \frac{hc}{mc^2}(1 - \cos\theta); \tag{5.32}$$

The constant quantity

$$\lambda_e = \frac{hc}{m_ec^2} = 2.4263102367(11) \times 10^{12}\ \text{m} \tag{5.33}$$

is called the *Compton wavelength of the electron*, where m_e is the electron mass and h is Planck's constant. The two digits in parenthesis represent the experimental error on the previous two digits. So far we have only used relativistic kinematics: nothing is said about the *interaction* between the photon and the electron: the above discussion is valid no matter what interaction is involved. The interaction enters into play when we calculate the cross section, i.e. the probability of the Compton scattering. This was done by Klein and Nishina in 1928.

5.6 The Cross Section for Compton Scattering

Klein[2] and Nishina[3] in 1928 calculated for the first time the Compton cross section using quantum mechanics.

$$\frac{d\sigma}{d\Omega} = \frac{1}{2}\alpha^2 r_c^2 P^2(E_\gamma, \theta)\left[P(E_\gamma, \theta) + \frac{1}{P(E_\gamma, \theta)} - 1 + \cos^2\theta\right] \tag{5.34}$$

where $d\Omega = \sin\theta\, d\theta\, d\phi$ and

$$P(E_\gamma, \theta) = \frac{1}{1 + (E_\gamma/m_ec^2)(1 - \cos\theta)} \quad \text{and} \tag{5.35}$$

[2]Oskar Klein (1894–1977), from Sweden. He's also known for the Kaluza–Klein theories, which speculate the existence of additional space dimensions.

[3]Yoshio Nishina (1890–1951) from Japan. He also discovered the isotope ^{237}U.

$$r_c = \frac{\hbar c}{(2m_e c^2)} \tag{5.36}$$

is the "reduced" Compton wavelength of the electron, ($\hbar = h/2\pi$) is the "reduced" Planck's constant and

$$\alpha = \frac{e^2}{4\pi\epsilon_0 \hbar c} \approx 1/137 = 7.297 \times 10^{-3}, \tag{5.37}$$

We call $\alpha = \alpha_{\mathrm{EM}}$ the *fine structure constant* for the electromagnetic interaction. It depends on the electron charge e, it is a dimension-less number, which gives the "strength" of the electromagnetic interaction, and its value is totally independent of the unit system we use.

$\epsilon_0 = 8.854 \times 10^{-12}$ F/m is the permittivity of vacuum.

> Note how the Klein and Nishina formula for the differential cross section of the Compton scattering *depends on the fourth power of the electric charge*, while the electric charge does not appear in the kinematic formulas of Compton scattering.

The K-N formula gives the angular dependence of the cross section: it gives the probability that a photon is scattered at a given angle. As we have seen already for the kinematic of the scattering, the process only depends on one angle: the one between the initial and the final direction of the photon. We say that there is a *cylindrical symmetry* around the axis of the initial photon direction. In other words, the probability of scattering along the azimuth angle ϕ is uniform. Note also that the cross section decreases when the photon energy E_γ increases. The cross section is referred to each scattering centre, i.e. electrons; so we need to multiply it by Z to obtain the Compton cross section for a material, as in Eq. (5.6).

5.7 Heavy Charged Particles

In this case the mass of the "projectile" particle is much larger than the mass of the "target" particle in the material, which is mostly electrons. This means we are dealing with protons, alpha particles or muons, or other particles which we'll meet later.

The incoming charged particle loses part of its kinetic energy in a series of many interactions. In each of them the projectile transmits a small part of its kinetic energy to the electrons in the target. The incoming particle is also deviated slightly from its initial direction. The term *multiple scattering* is used to indicate this effect. The Bethe-Bloch formula, below, describes the energy loss per unit of length of a heavy

charged particle when colliding with the electrons in a medium:

$$-\left\langle \frac{dE}{dx} \right\rangle = \left(\frac{e^4}{4\pi\epsilon_0^2} \right) \frac{z^2}{m_e v^2} (Z\mathcal{N}) \ln\left(\frac{2m_e v^2}{I} \right) \tag{5.38}$$

This is the non-relativistic version of the formula, which is valid for a kinetic energy of the particle in the interval from 0.5 to 500 MeV, when dealing with protons, alpha particles or *mesons*. This formula is calculated in many, and more advanced, textbooks (Cerrito 2017; Fernow 1986; Segré 1977). We can use it as a starting point to highlight the features of the passage of electrically charged particles.

The electron electric charge e is present in the formula, because the energy loss is due to electromagnetic interaction and, once again, it enters to the fourth power, just like in Compton scattering cross section. The electric charge of the projectile z (in units of e) enters the formula quadratically, so an alpha particle loses 4 times its energy with respect to a proton of the same velocity v; this also enters the formula quadratically and is measured with respect to the target, which is at rest. Z indicates the atomic number of the target, or the number of electrons per atom and enters linearly in the formula, like the atomic density of the material (Eq. (5.4)), which is indicated with $\mathcal{N}$. In other words the term $(Z\mathcal{N})$ is the average electron density. The parameter I is the average ionisation energy of the target, and is shown in Fig. 5.10

Felix Bloch (1905–1983) from Switzerland was awarded the Nobel prize in 1952 for his work on precision measurements of nuclear magnetic moments. He was the first director general of the European laboratory CERN.

as a function of Z. These collisions occur between the charged particle and the electrons in the target atoms and therefore the electron mass m_e is the only mass

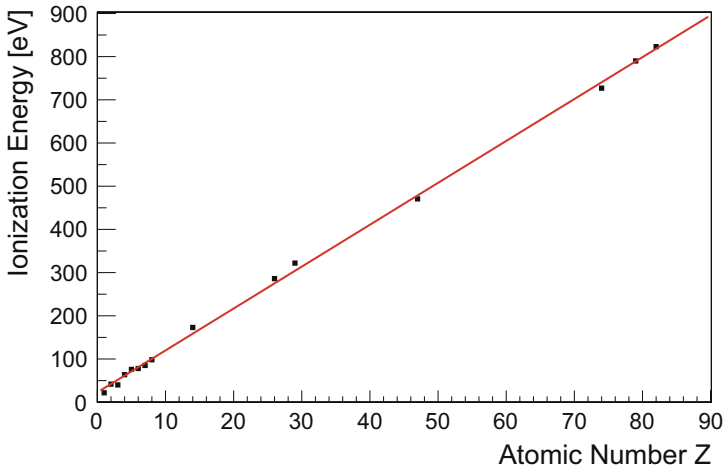

Fig. 5.10 Average ionisation energy as a function of the atomic number. The line represents a fit to the data: $I \approx 22.8 + 9.7Z$

appearing explicitly in the formula. In general also in this case the density of the material is factored out and $1/\rho \langle dE/dx \rangle$ is called the *stopping power*. The mass of the projectile particles, m_p, appears if we re-write Eq. (5.38) in terms of the kinetic energy $E = 1/2 m_p v^2$ of the incoming particle:

$$-\frac{1}{\rho}\left\langle \frac{dE}{dx} \right\rangle = K \frac{m_p}{m_e} \frac{1}{E} \frac{z^2 Z}{M} \ln\left(\frac{4 m_e E}{m_p I}\right) \tag{5.39}$$

where

$$K = 2\pi\, \alpha^2 \hbar^2 c^2 N_A \;=\; 0.078 \text{ MeV}^2 \text{ cm}^2$$

It is clear that at constant density, materials with higher Z have a higher stopping power. For higher energies, the Bethe-Bloch formula has to be corrected by a relativistic factor γ^2 inside the logarithmic term, which gives rise to an increase of energy loss with the particle energy. The energy loss is minimum for charged particles in the interval 0.1–1 GeV, which are called *minimum ionising particles*.

At even higher energies radiative losses become important, with a mechanism which is very important for electrons. Another clear limitation of Eq. (5.39) is evident in the low kinetic energy limit, where the logarithmic term would become zero and then negative, which is unphysical. Therefore, there is an intrinsic cut-off, which depends on the ionisation energy. Equation (5.39) which is plotted in Fig. 5.11 for muons in copper and Eq. (5.38) have to be used with care. The stopping power of copper for *muons* is shown in Fig. 5.12, for a large energy range. In this figure all effects and corrections are taken into account.

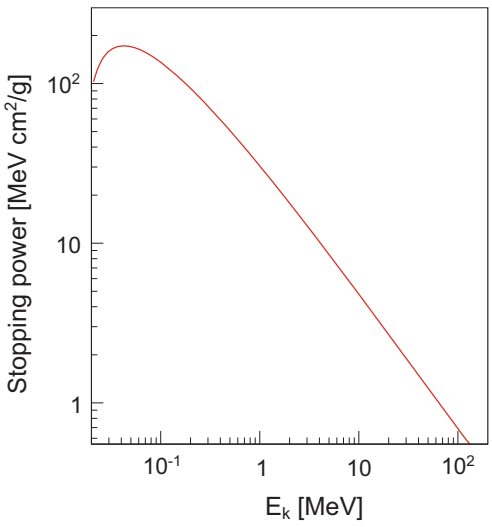

Fig. 5.11 The simplified form of the Bethe-Bloch formula, Eq. (5.39), can be used to calculate the energy loss of muons in copper, within its interval of validity: as long as the particle is non-relativistic and its kinetic energy is not too low. The results of the calculation of the muon stopping power for copper is shown as a function of the muon kinetic energy

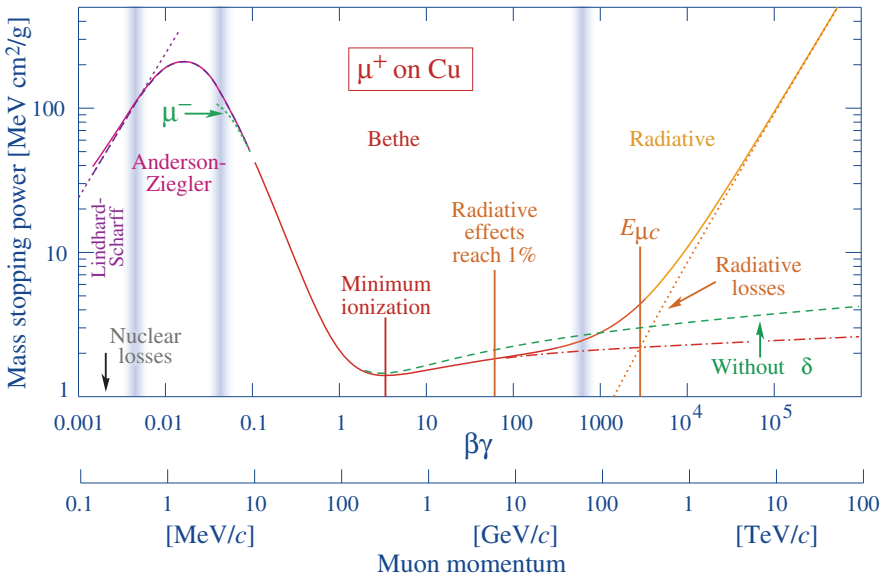

Fig. 5.12 Specific energy loss in copper for muons as a function of their initial momentum. Reprinted with permission from M. Tanabashi et al. (Review of Particle Physics), Phys. Rev. D, vol. 98-1, p. 447 (2018). Copyright (2018) by the American Physical Society. Muons have a mass about 200 times larger than electrons and are electrically charged. To obtain the energy loss per unit of length the values on the y axis have to be multiplied by the copper density

In case of charged particles traversing a material, their flux remains constant, but the kinetic energy of each particle decreases. This is very different from the case of photons, whose number decreases exponentially inside the material. In case of thick absorbers, particles can lose all their energy inside the material and come to a rest after a well-defined *range* R which depends on their initial kinetic energy E_k. To calculate the range we need to integrate Eq. (5.38) from E_k to zero kinetic energy. The logarithmic term makes the analytic integration difficult, but above a certain initial energy it just adds a constant. If we consider the logarithmic term as a constant we have:

$$R = \int_{E_k}^{0} dE \frac{1}{\langle -dE/dx \rangle} \approx \text{Const} \int_{E_k}^{0} E\, dE = {}^1\!/_2\, \text{Const}\, E_k^2 \tag{5.40}$$

In the energy range where the average energy loss varies with the kinetic energy as $1/E$, the range of the particle increases quadratically with its energy. Writing explicitly the entire formula, and using the log of the average energy, from Eq. (5.39) we obtain:

$$R \approx \frac{1}{2\,K} \frac{m_e}{m_p} \frac{M}{Z\rho} \frac{1}{z^2} \left[\ln\left(\frac{2 m_e E_k}{m_p I} \right) \right]^{-1} E_k^2\ ; \tag{5.41}$$

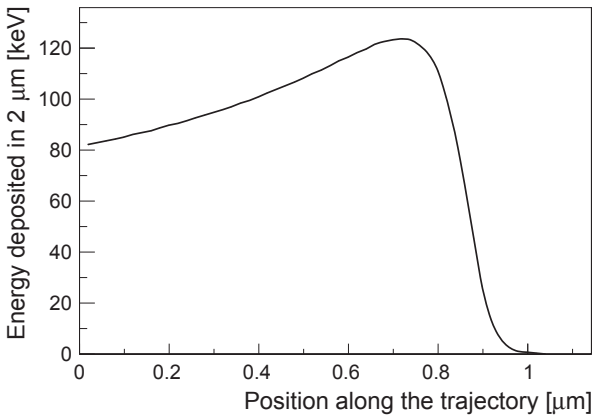

Fig. 5.13 Energy deposition as a function of the position along the trajectory for 5 MeV α-particles in copper. Most of the kinetic energy is deposited in a narrow layer near the end of the particle trajectory. This feature is used in hadron therapy, where the peak is much more pronounced, and in medical applications of α-emitting radionuclides. The curve is named after William Henry Bragg (1862–1942), from England, he taught physics in Adelaide, Australia, for 20 years, then in Leeds and London. He was awarded the Nobel prize in 1915 with his son Lawrence for their research on X-ray diffraction in crystals

the range is inversely proportional to the density of the material, as expected. This formula has its own limitations: for instance, it calculates the path length, but the trajectory is not a straight line, so we don't obtain the depth in the material where the particle would stop. However, it can be used to calculate the upper limit of the range of α particles in air or β particles in Al. For practical applications, like doping of semiconductor materials by ion implantation, more refined calculations are implemented in computer-based simulations.

The energy loss per length of the path is larger as particles progressively lose their energy, as is evident from the $1/E$ term in Eq. (5.39). Therefore, most of their energy is lost at the end of the path, where their kinetic energy is lowest. Plotting the specific energy loss as a function of the penetration depth we obtain the characteristic *Bragg curve*, which has a peak of energy deposition near the end of the particle trajectories, as shown in Fig. 5.13. This feature is used in hadron therapy, where a beam of protons is aimed at a cancer and its energy is tuned to have the protons stop inside the cancer volume, where most of its energy is delivered. For the same reason α-emitting radionuclides for medical treatment are more effective in delivering high dose to cancer cells than the γ-emitting nuclides.

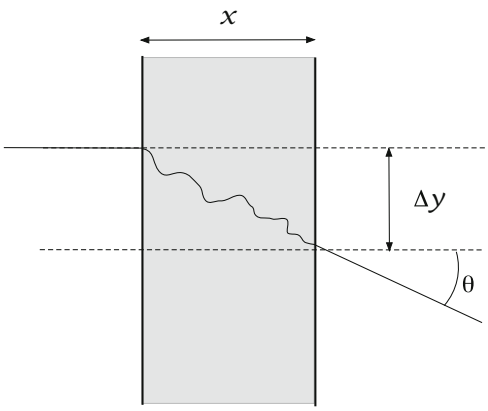

Fig. 5.14 Multiple scattering of charged particles traversing a material: they are deviated from their initial direction by an angle θ which depends on the material and on its thickness x

5.8 Charged Particles Traversing Thin Layers

Electrically charged particles lose kinetic energy by a large number of electron scattering events. After traversing a thin section of material the charged particles emerge with an angle θ with respect to the original direction (Fig. 5.14). The distribution of these angles is approximated by a Gaussian, and its standard deviation is inversely proportional to the particle momentum and proportional to the square root of the material thickness.

The energy loss distribution in thin layers, however, does not follow a Gaussian distribution. The reason is that occasionally scattering events occur with a large energy loss. The resulting distribution is skewed, with the average energy loss being considerably larger than the most probable energy loss. The average energy loss is still what calculated with Eq. (5.38), but the most probable energy loss is a more significant parameter. The distribution is described by the following integral function:

$$\phi(x) = \frac{1}{\pi} \int_0^\infty dt \exp(-t \log(t) - xt) \sin(\pi t) \tag{5.42}$$

This is the so-called Landau distribution; it is a slightly complicated function: the variable x representing the energy loss is inside the integral and the function has no free parameter. The shape of the distribution is shown in Fig. 5.15. It reproduces well the energy loss in thin materials, as long as they are not extremely thin. In these cases the Landau distribution is considerably wider than the experimental distribution and better distributions have width and most probable value as parameters. The energy loss distribution is also called *straggling distribution*.

The distribution is named after Lev Davidovich Landau (1908–1968) from Russia. He was awarded the Nobel prize in 1962 for his work on superconductivity. He is also known for his textbook on theoretical physics, in ten volumes, written with Evgeny Lifshitz.

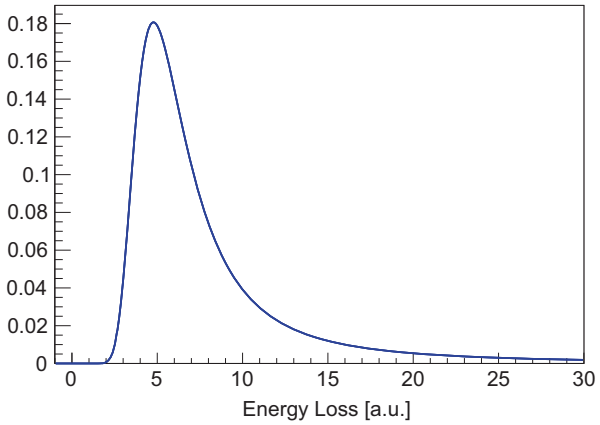

Fig. 5.15 The Landau distribution describes the energy loss of charged particles in thin absorbers, where they lose only a small fraction of their kinetic energy. Its analytical form is shown in Eq. (5.42). For very thin absorbers this formula slightly underestimates the width

5.9 Electron Energy Loss

Electrons have the peculiarity that are identical to the main target they interact with in the matter: other electrons.

Because of their small mass, electrons are subject to a large deceleration and emit a considerable electromagnetic radiation, which is called bremsstrahlung, German for "braking radiation". When they interact with other electrons both particles emit braking radiation, which interferes destructively at large distances. However, when they scatter off the electric field of atomic nuclei their acceleration emits electromagnetic radiation. The energy loss per unit of length, by radiation only, is given by the following formula:

$$-\left(\left\langle\frac{dE}{dx}\right\rangle\right)_{\text{rad}} \approx \frac{4\mathcal{N}Z^2\alpha^3(\hbar c)^2}{m_e^2c^4}E\ln\frac{183}{Z^{1/3}} \tag{5.43}$$

where $\mathcal{N} = \rho N_A/M$ and N_A is the Avogadro's number, $\alpha \approx 1/137$, A and Z are the mass and atomic number of the target, E is the energy of the electron and $\hbar = h/2\pi$ and m_e is the electron mass. As above, we can just note some features, e.g. that this cross section increases linearly with the electron kinetic energy E.

We define the *critical energy of an absorber* E_c as the electron energy above which the energy loss by radiation is larger than the energy loss by ionisation. It

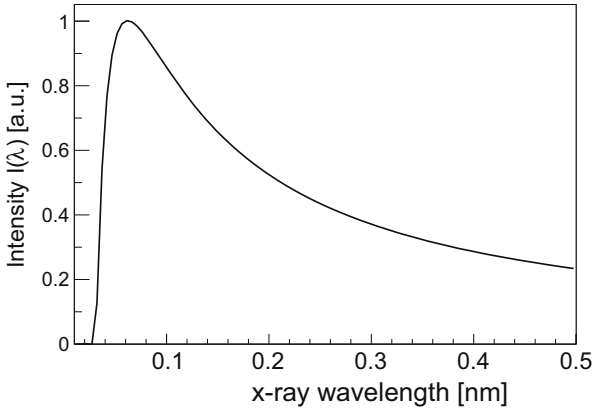

Fig. 5.16 The wavelength λ of the X-rays emitted by bremsstrahlung has a continuous distribution. The wavelength distribution of X-rays emitted by 40 keV electrons is calculated with Eq. (5.45) and shown here

varies as $E_c \propto Z^{-1}$: for solid material an approximate function is

$$E_c \approx \frac{610}{Z + 1.24}\,\text{MeV} \tag{5.44}$$

and its values are in the range 5–350 MeV. Low-energy electrons, such as those produced by radioactive sources or used in cathode ray devices, lose most of their energy by ionisation; however, braking radiation is never completely negligible.

The braking radiation is emitted in the X-ray range: energetic electrons, when interacting with the matter, transform part of their kinetic energy into electromagnetic radiation. This mechanism occurs in X-ray tube generators. The emitted X-ray spectrum depends on the electron initial energy E_0, but has a universal shape, which is given by the Kramers' law:

$$I(\lambda)\,d\lambda = k\frac{iZ}{\lambda^2}\left(\frac{\lambda}{\lambda_{\min}} - 1\right)d\lambda; \quad \text{where } \lambda_{\min} = \frac{h\,c}{E_0} \tag{5.45}$$

and $I(\lambda)\,d\lambda$ is the X-ray intensity at wavelength λ, i is the electron intensity. The shape of the wavelength spectrum is shown in Fig. 5.16.

At high wavelengths, the emission of X-rays is collinear with the electrons, and is absorbed by the same material and by any other material which may be present. This changes dramatically the spectrum shape at high wavelengths. At low electron energy ($E_0 < m_e c^2$) the emission of X-rays is maximum in the direction perpendicular to the electron beam and is polarised with the electric field oscillating along the electron direction. At higher energies ($E_0 \gg m_e c^2$) the radiation is emitted mostly along the initial direction of the electrons. As X-ray detectors are

normally calibrated according to the energy, rather than wavelength, we can change variables in Eq. (5.45) and obtain the energy spectrum

$$\lambda = \frac{h\,c}{E};\quad d\lambda = \frac{h\,c}{E^2}\,dE$$

$$I(E)dE = k\frac{iZ}{h\,c}\left(\frac{E_0}{E} - 1\right)dE \tag{5.46}$$

It should be noted at this point that the bremsstrahlung cross section has a so-called *infrared divergence*, meaning that an infinite number of photons with infinitesimal energy are emitted. As the total energy loss is finite, we need to introduce, from a theoretical point of view, a photon cut-off energy below which the interaction can be ignored. This process is not the only one to require such a mathematical treatment.

In addition to generating braking radiation, electrons also ionise the atoms, just like other charged particles. Electrons from the outer shells make a transition and occupy the inner shells or energy levels which have been left empty by the ionisation process, emitting electromagnetic energy, i.e. photons. The photon energy depends on the difference between the energy levels of the atoms. Therefore the material emits also a characteristic X-ray radiation, which depends on the material which is irradiated. The resulting spectrum is shown in Fig. 5.17, where the following effects are calculated:

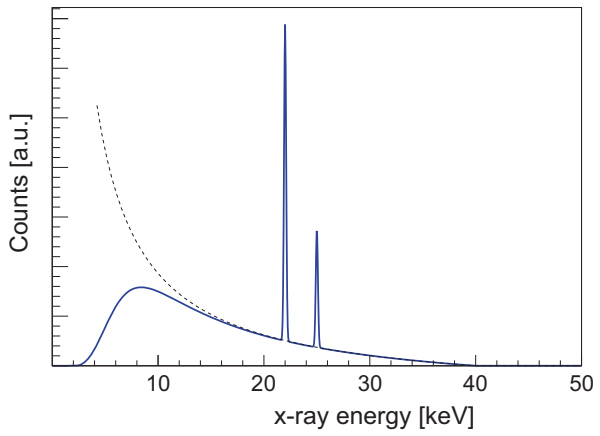

Fig. 5.17 Calculated energy spectrum of X-rays emitted by an X-ray tube with silver anode operated with 40 keV electrons. The bremsstrahlung spectrum is calculated with Eq. (5.46). The low-energy X-rays are absorbed by the anode itself and by the glass window; the absorption cross section is assumed as $\sigma_{\mathrm{pe}} \propto 1/E_\gamma^3$. The shape of the un-filtered spectrum is shown as a dashed curve. The silver K_α and K_β lines are added as narrow Gaussian distributions. Compare it with the experimental spectrum shown in Fig. 5.23

– Bremsstrahlung emission, as in Eq. (5.46),
– Absorption of low-energy X-rays by the material itself and by the glass window,
– Emission of K lines by the material, which we assume to be silver.

5.10 Neutrino Interactions with Matter

Neutrinos will be introduced more formally in the next chapter, but we have already encountered them in describing the β decay. They are electrically neutral particles and their mass is not precisely measured, it is extremely small, but not zero. The present limit for all three types of neutrinos is at about $m_\nu < 1\,\text{eV}$. They only interact with matter with the weak interaction. A feature of this interaction is that the cross section increases with the neutrino energy, up to very high energies. Nevertheless, the cross sections for various processes involving neutrinos range from 10^{-28} to 10^{-17} barn for energies in the range from 100 eV to 1 GeV. As a comparison, the Compton cross section in lead ($Z = 82$) is of the order of 10 barn (Fig. 5.6), which makes the cross section per electron 16 orders of magnitude larger. The energy loss mechanisms of neutrinos would be similar, in principle, to the energy loss of charged particles, but the multiple scattering occurs on a much larger scale, due to the extremely small cross section.

We can look back at the equation describing the photon attenuation, Eq. (5.11). Independently from the fate of the impinging particle, it describes the distribution of the depth of its first interaction with the matter; the parameter $1/\mu$ is the mean path before interaction. Using the largest value of neutrino scattering cross section, for a kinetic energy in the $\approx$ 1 GeV range (10^{-17} barn), in Eq. (5.11) the neutrino mean free path in iron is:

$$\mu_\nu = \rho \frac{N_A}{M} \sigma \ ;$$

$$\mu_\nu(Fe) \approx 7.87 \frac{\text{g}}{\text{cm}^3} \times \frac{6.022 \times 10^{23}\,\text{mol}^{-1}}{55.84\,\text{g mol}^{-1}} \times 10^{-17} \times 10^{-24}\,\text{cm}^2$$

$$\mu_\nu(Fe) \approx 8.5 \times 10^{-19}\,\text{cm}^{-1};\ 1/\mu_\nu = 1.2 \times 10^{18}\,\text{cm} = 1.2 \text{ light years}$$

The actual cross section can be slightly larger than that, if other processes are taken into account, but it does not change the fact that neutrinos with a kinetic energy up to about a GeV can pass through about one light-year of dense matter without interacting at all. The very small cross section makes it very difficult to study neutrinos, requiring a large mass of active detectors and a large intensity of neutrinos to record a small number of neutrino interactions. On the other hand, it makes it possible to study neutrino oscillations with neutrinos produced in an accelerator and traveling long distances, of the order of thousands kilometers, without needing any kind of vacuum pipe or tunnel.

The first observation of anti-neutrinos occurred with the reaction:

$$\overline{\nu}_e + p \rightarrow n + e^+ \tag{5.47}$$

which is sometimes called "inverse beta decay"; the measured cross section[4] was

$$\sigma(\overline{\nu}_e p \rightarrow n e^+) = (11.0 \pm 2.6) \times 10^{-44}\,\mathrm{cm}^2$$

A neutrino flux $\Phi \approx 5 \times 10^{13}\,\mathrm{cm}^{-2}\,\mathrm{s}^{-1}$ obtained from a nuclear reactor was used to detect neutrinos for the first time.

Although neutrinos are able to ionise, for their extremely low cross section they are not considered as ionising radiation for all practical purposes.

5.11 Passage of Radiation from the Point of View of the Material

The energy deposited by radiation in a material has three effects: ionises the material; increases locally its temperature; generates other radiation, which can be absorbed by the material or escape it. An electron from photoelectric effect may ionise other atoms, but also leaves behind a ionised atom, which receives an electron from the environment and will emit X-rays, which can be absorbed photoelectrically by neighbouring atoms and so on. Charged particles leave tracks of ions in the material, but protons and *mesons* and heavy ions at a sufficiently high energy can also displace atoms from a crystal lattice.

The total amount of radiation energy deposited per unit of mass in a material is measured in Gray (Gy) and is also called *absorbed dose*

$$1\,\mathrm{Gy} = 1\,\mathrm{J/kg} = 6.24 \times 10^{12}\,\mathrm{MeV/kg} \tag{5.48}$$

Of course, only the part of material which is interested by the radiation has to be accounted for in the mass value. This is especially important if the radiation is completely stopped, like in the case of charged particles. Large radiation doses can damage solid material, induce or accelerate chemical reactions, accelerate ageing.

5.12 Particle Detectors

Ions separated by radiation can be transformed directly or indirectly into an electric signal, or in some case into a permanent chemical change to detect ionising

[4]Frederick Reines and Clyde L. Cowan, Jr., *Measurement of the free antineutrino absorption cross section by protons*, Phys. Rev. 113 (1959), p 273.

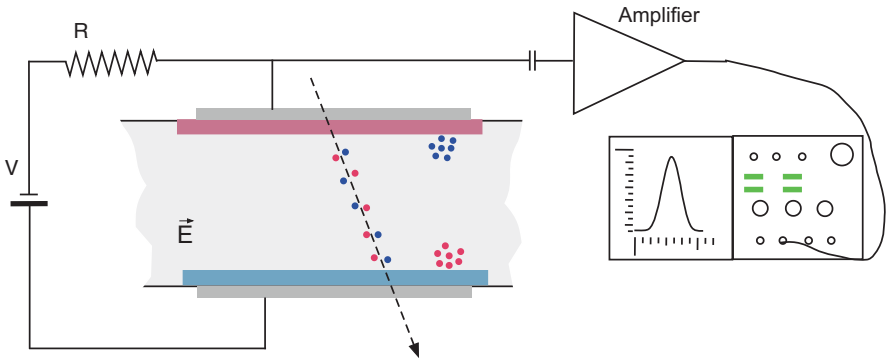

Fig. 5.18 Schematics of a typical solid-state detector. The material is a semiconductor, with a junction on one surface and a highly doped layer on the other surface. The typical thickness is 0.1 to 0.5 mm. The electrodes can also have the shape of strips or pixels, for spatial resolution. The electric charges are separated by the radiation and drift in the electric field of a reverse-biased diode structure. This generates a current, which is amplified by an external circuit and can be observed with an oscilloscope. Positive ions in semiconductor crystals are called *holes*: the lack of electrons move like bubbles in a liquid towards the negatively charged electrode

radiation. This happens in X-ray films, where the radiation ionises crystals of AgBr; the subsequent chemical treatment removes bromine, leaving metallic silver as a dark area in the film only in the areas which have been exposed to radiation.

In solid-state detectors, charged particles lose their energy, which partially goes into crystal excitations, i.e. phonons, and partly to generate electron-hole pairs. On average 3.6 eV is needed for a single pair in silicon, and a signal of $\approx 3 \times 10^4$ electrons can be generated by a minimum ionising particle. Electrons and positive ions ("holes") drift in an electric field in a reverse-biased diode structure and generate a current pulse, which is amplified electronically, as sketched in Fig. 5.18. In this case the distribution of pulse heights is proportional to the distribution of energy loss. For thin detectors it is a modified Landau distribution.

In gas-operated detectors the same mechanisms are in place, but the energy loss in a gas is typically smaller than in solids, because of the density factor. A smaller electric charge is produced. To have a detectable electric signal the method of charge amplification with gas discharge is used: the primary electrons, i.e. those generated by radiation, are drifted to a small sized electrode, like a tiny wire; in its vicinity the electric field is large enough that electrons acquire energy to ionise other molecules of the gas. The resulting electric signal can be furtherly amplified with external electronic circuits. When the internal amplification factor, which is controlled by the voltage and diameter of the wire and by the gas pressure, is relatively small the signal amplitude is proportional to the initial ionisation. The detector is called a *proportional chamber*. When the gas gain is large we have the Geiger counters.

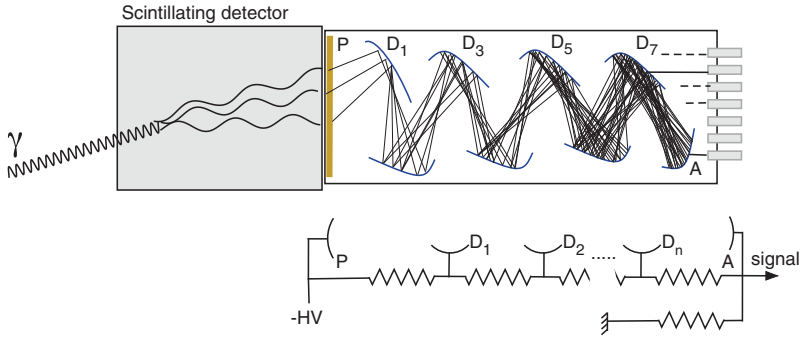

Fig. 5.19 Schematics of a scintillator coupled to a photomultiplier: a scintillator detector (S) produces flashes of light when hit by ionising radiation; light is transmitted through a window to the vacuum tube where a photocathode (P) emits an electron for every photon; electrons are amplified by secondary emission in the various dynodes (D_n); the electric signal is collected at the anode (A)

The Geiger tube is named after Hans Geiger (1982–1945) from Germany, who worked from 1907 to 1912 with E. Rutherford in Manchester, UK and then taught in Tubingen and Berlin, Germany.

A third important class consists of scintillating detectors: all materials emit photons when they are ionised and the electric charges recombine; in the majority of cases the light is also re-absorbed; in scintillator materials this light can be transmitted over a large distance and collected by a light-sensitive electronic device, to be transformed into electric signals. In general, scintillating detectors are made of two-component materials: a light-transparent material which hosts a lower concentration of photoluminescence centres that emit at a wavelength which is not attenuated by the hosting material. An example is thallium in sodium iodide crystal. The energy from primary electrons activates the photoluminescence centres, which produce very small flashes of light, which is detected by a device called a *photomultiplier*, as sketched in Fig. 5.19. Scintillating detectors can be solid inorganic, as NaI(Tl) or solid organic, like plastic scintillators, or liquid. Scintillators are also used to enhance the sensitivity of photographic films to X-rays, as shown in Fig. 5.22.

Detectors can be used to measure particle energies, or the position where particles hit the detectors, e.g. for imaging, or also the time when particles hit the detector. For each application there are advantages and disadvantages of the various technologies. One parameter which is common to all detectors is the efficiency, which is calculated as the fraction of incident radiation which gives an electric signal which is recognised as such. Energy resolution is an important parameter, especially

for spectroscopy. Particle detectors are used to measure the energy of the radiation emitted by radionuclides, which is their identifying "fingerprint". In this case the energy resolution is a very important parameter.

5.13 Biological Effects of Radiation

Energy deposited by radiation in living cells has the same effects of creating ions, increasing the temperature locally and generating other radiation. Ionising the saline solution inside cells or the water between cells creates free radicals, which are chemically very reactive. Their presence may have several effects: from killing cells to generating mutations, including carcinogenic ones. The effect of radiation in a living tissue is measured by the absorbed energy weighted by a factor that takes into account how this energy is distributed. This is the *equivalent radiation dose* and is measured in Sievert (Sv), The factor W_R depends on the radiation type and ranges from 1, for gamma rays, to 20 for α particles and heavy ions:

$$\text{Equivalent radiation dose} = \text{absorbed dose} \times W_R; \tag{5.49}$$

$$1\ \text{Sv} = 1\ \text{Gy}\ \times W_R$$

Living cells have natural repair mechanisms to the radiation effects, it is also very important to consider the time interval in which this dose is delivered, which is the *equivalent dose rate*, in Sievert per hour (Sv/h) or per year (Sv/y). The same dose has the highest effects if it is delivered in a short time. Radiation is used to kill germs and sterilise equipment and food. It is also used to kill cancer cells: radiotherapy uses alpha and beta-emitting radionuclides linked to molecules which are attracted to cancer cells; hydrotherapy uses collimated beams of charged particles with tunable energy, so that the position of the Bragg peak corresponds to the depth of the tumour. The same radiation, if administered to healthy organs, will kill their cells in exactly the same way and may also cause cancer. An equivalent dose of 1 Sv corresponds to a 5.5% probability of developing cancer from radiation.

We are constantly exposed to natural radiation, from cosmic rays, from radon gas, from other radioactive minerals, like ^{40}K. In general, we absorb an equivalent dose of approximately 1.5–5 mSv/y from natural sources, depending on the location where we live: it is mainly linked to geology and altitude. In Europe the limit on the effective dose for occupational exposure is presently 20 mSv/y. For all manipulation of radioactive sources or operation of X-ray equipment the principle of reducing all unnecessary exposure must be applied.

Other units of exposure are the *rem*, which originally stands for Röntgen equivalent for men: 1 rem = 0.01 Sv. It is now based on the *rad*: 1 rad = 100 Gy. These units are presently officially used only in the USA.

5.14 Radiography

To obtain X-ray images of objects or parts of our body (Fig. 5.20), the object is placed between a X-ray tube and an imaging detector, which can be a special photographic film or an electronic detector. What we see is the shadow of the object projected onto the detector. At a given X-ray energy or wavelength, materials of different Z have different absorption coefficients: while water and other tissue can be transparent, bones which contain calcium absorb the X-rays and project a shadow onto the film.

The ideal generator would produce single-energy X-rays from a point-like source at large distance from the object, in such a way that the rays can be considered as parallel to each other, and objects project a sharp "shadow". The ideal detector has

Fig. 5.20 Shadow of a human hand projected on an X-ray detector. The part in black the film has been hit by X-rays, while the parts which have remained white have been shadowed by the bones, which have absorbed the X-rays

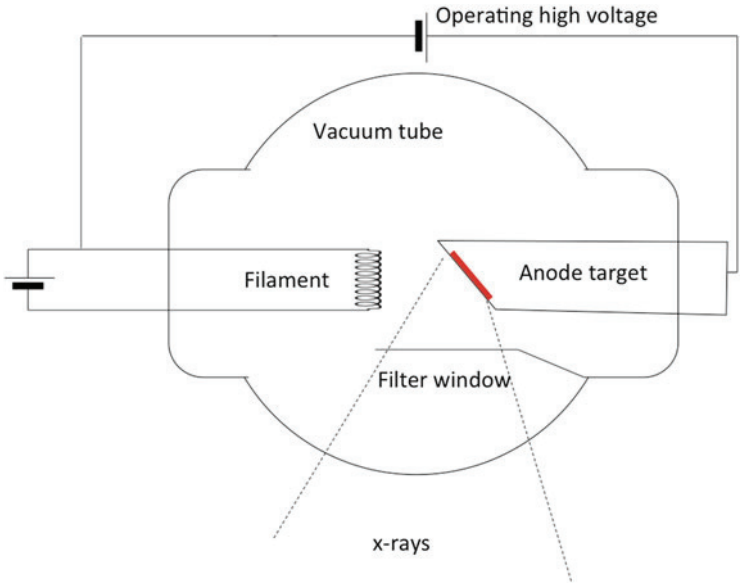

Fig. 5.21 Schematics of an X-ray tube. Electrons are produced by an incandescent filament in vacuum; the production process is called *thermionic emission*; they are accelerated with the high voltage to the desired energy. When they hit the cathode they produce a continuum spectrum due to bremsstrahlung, but they also ionise the cathode atoms. When the electron energy is larger than the K energy levels, occupied by the innermost electrons, also the characteristic X-ray fluorescence lines of the cathode material are emitted. These lines are monoenergetic. Depending on the application, the lower part of the spectrum may be intentionally suppressed by a filter, to reduce the dose to the patient and to minimise the energy dispersion. The cathode is heated by the electron current, which may reach 1 A. A rotating cathode is sometimes used for high intensities. The cathode is inclined, because the X-ray emission is maximum in the direction perpendicular to the electron velocity. To avoid penumbra effects on the film, the electrons are focused to reduce the size of the X-ray source

100% efficiency, a granularity of the order of micrometres and a linear response over several orders of magnitude. The aim is to have an excellent resolution, maximum contrast, while minimising the radiation dose to the patient. In reality an equipment is the best available compromise. Operating voltages range from 25 to 140 kV, anodes are typically made of tungsten, for general purpose, or molybdenum for soft X-ray mammography. Their K-level emission lines are $E_\gamma = 69.5$ and 20 keV, respectively. Currents can reach 1 A and the lower part of the spectrum ($E \leq E_\gamma$) is filtered out to minimise the dose to the patient.

The detector can be a simple, but specific, photographic film, which may have an enhanced detection efficiency by using a scintillator device, which converts X-rays into light. Digital radiography uses either a light-sensitive device to detect scintillation light, or pixelated detectors which convert directly X-rays into electric signals and then into an image. This gives immediate feedback, without any chemical processing of the film. A sketch of the devices is shown in Figs. 5.21 and 5.22.

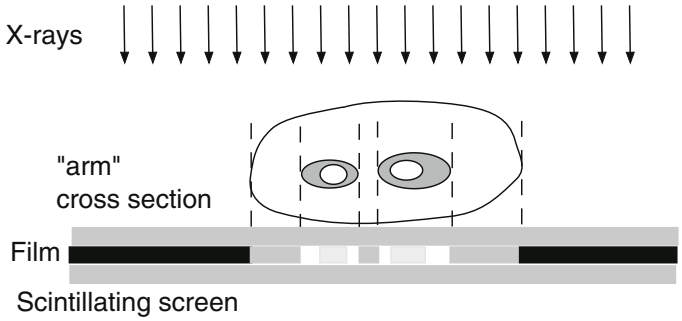

Fig. 5.22 Cross section sketch of an arm in contact with a radiology film detector. Two layers of scintillating material are used to enhance the sensitivity to X-rays of the photo-sensitive film. Black areas correspond to areas which were exposed to the X-rays, light areas are those in the shade of material with high Z, like bones. The contrast depends on the difference of absorption coefficients (μ) of the various materials at the dominant X-ray energy. Electronic detectors can replace the film and lower the dose to the patient

The unavoidable Compton scattering inside the object, or patient, deflects the incoming X-rays and reduces their energy, adding a noise component to the image and decreasing the contrast. Special collimators can be used to reduce this effect, at the price of efficiency, while energy-sensitive detectors can be used to filter out Compton-scattered photons.

5.15 Problems

5.1 A case study: an X-ray tube operates in the range 25–140 kV. Calculate the range of 40 keV electrons hitting a silver anode. ($\rho = 10.5$ g/cm^3, $M = 107.87$ g/mol). For this study we can in first approximation neglect the energy lost by radiation. Will the obtained value be larger or smaller than the real one? Assume a current of 10 mA, calculate the energy loss in 1 s in the anode and compare this value with the purely electrical power. Assuming no heat exchange, a mass of the anode $m_a = 20$ g, and a heat capacity $C_h = 25$ J/mol/K, calculate the temperature of the anode after 10 s of continuous operation.

5.2 A radiology lab uses 40 keV X-rays from an apparatus with a silver anode, whose measured emission spectrum is shown in Fig. 5.23. The walls of the lab need to be thick enough to contain the radiation. What thickness of lead is needed to attenuate the radiation intensity to 0.1% of the initial value?

What thickness is needed if we use concrete instead?.

The energy of the Ag emission lines K_β and K_α and the corresponding attenuation coefficients for lead are reported in Table 5.1. The lead density is 11.3 g/cm^3. Should we use the k_β or the spectrum end-point energy? The attenuation coefficient for concrete at 40 keV is 0.5 cm^2/g and its density is 2.4 g/cm^3.

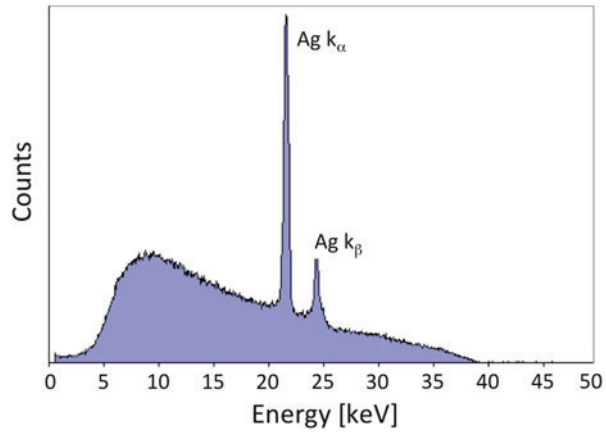

Fig. 5.23 Spectrum of X-rays emitted by a tube with silver anode, operated at 40 kV and measured with a CdTe detector (Courtesy Amptek, Inc. www.Amptek.com)

Table 5.1 Table of the X-ray attenuation coefficients in lead, for three values of the X-ray energy

Line	E (keV)	$\mu(\text{cm}^2/\text{g})$
k_α	22	70
k_β	25	45
Bremsst.	40	14

5.4 Calculate the range of 5 MeV α particles ($z = 2$) in nitrogen at standard conditions, which is an approximation for air, with density $\rho = 1.2\text{mg/cm}^3$, $Z = 7$ and atomic mass $M = 14.00$ g/mol. The mass of an α particle is $m_\alpha = 3727.3\ \text{MeV/c}^2$.

5.5 A radioactive source of ^{90}Sr emits β^- with an end-point of 546 keV. Calculate the range of electrons in aluminium, neglecting radiative energy losses. What thickness of aluminium would shield 99% of all radiation, including bremsstrahlung? Aluminium: $M = 26.98$ g/mol, $\rho = 2.7\ \text{g/cm}^3$.

5.16 Solutions

Solution to 5.1 First of all we verify that the kinematics of 40 keV electrons can be approximated by non-relativistic formulae, so Eq. (5.41) is valid. From Eq. (5.41) we first calculate the average ionisation energy $I = 22.8 + 47 \times 9.7 = 480$ eV

to be used in the average of the log term:

$$L = \ln\left(\frac{2 \times 511 \times 40\,\text{keV}^2}{511 \times 0.48\,\text{keV}^2}\right) = 4.42$$

we have:

$$R = 0.5 \times \frac{0.0016\,\text{MeV}^2}{0.078\,\text{MeV}^2\ \text{cm}^2}\,\frac{0.511}{0.511}\,\frac{107.00\,\text{g/mol}}{47 \times 10.5\,\text{g/cm}^3}$$
$$\times \frac{1}{4.42} = 0.0005\,\text{cm} = 5\,\mu\text{m}$$

This value is larger than the real depth of electrons because we have neglected the braking radiation and because the trajectory of electrons inside the material is not a straight line. However, we have an order of magnitude of a few micrometres of the anode which takes part to the X-ray emission. 10 mA= 10^{-2} C/s= $10^{-2}/1.6 \times 10^{-19} = 6.25 \times 10^{16}$ e/s. In 1 s the energy loss is

$$6.25 \times 10^{16} \times 40 \times 10^3 = 250 \times 10^{19}\,\text{eV} = 250 \times 10^{19} \times 1.6 \times 10^{-19} = 400\,\text{J}$$

The value of the electrical energy is

$$W = I\,V\,t = 10^{-2}\,\text{A}\ \times 40 \times 10^3\,\text{V} \times 1\,\text{s}\ = 400\,\text{J}$$

The temperature of the anode increases by ΔT

$$\Delta T = t \times \frac{W m_a}{M C_h} = 10\,\text{s} \times \frac{400 \times 10}{107.87 \times 25} = 14\,\text{K}$$

Even with a very modest current, the temperature of the anode increases considerably. This is the reason why rotating or water-cooled cathodes are used in industrial applications.

Solution to 5.2 As the photoelectric cross section for a given material decreases with the cube of the X-ray energy, we consider the maximum energy in the spectrum, which is 40 keV. The attenuation coefficient for lead is $\mu' = \rho\mu = 11.3 \times 14 = 158.2\,\text{cm}^{-1}$.

$$N(x)/N(0) = e^{-\mu' x} = 0.001;\ \ \Rightarrow -\mu' x = \ln(0.001);$$

$$x = -\frac{1}{\mu'}\ln(0.001) = 6.91/158.2 = 0.4\ \text{mm}$$

In case of concrete $\mu' = \rho\mu = 2.4 \times 0.5 = 1.2\,\text{cm}^{-1}$ and

$$x = -\frac{1}{\mu'}\ln(0.001) = 6.91/1.2 = 5.7\,\text{cm}$$

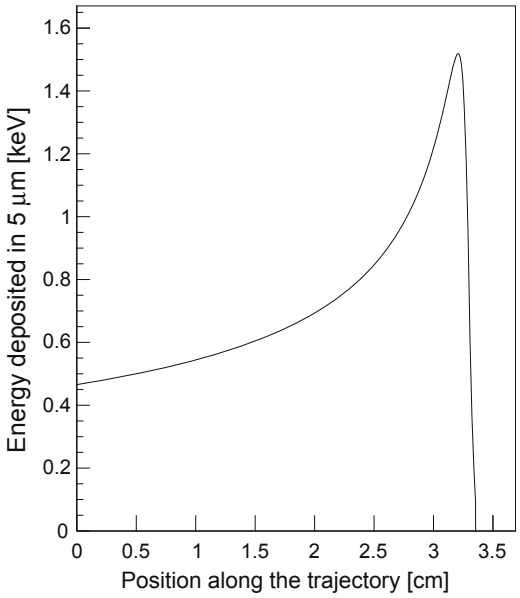

Fig. 5.24 Energy loss profile of 5 MeV α particles in air, as calculated with a numerical integration of Eq. (5.39)

Solution to 5.4 From Eq. (5.41) we first calculate the average ionisation energy $I = 22.8 + 7 \times 9.7 = 90.7$ eV to be used in the average of the log term:

$$L = \ln\left(\frac{2 \times 0.511 \times 5\ \text{MeV}^2}{3727.3 \times 9 \times 10^{-5}\ \text{MeV}^2}\right) = 2.86$$

we have:

$$R = 0.5 \times \frac{25\ \text{MeV}^2}{0.078\ \text{MeV}^2\ \text{cm}^2}\ \frac{0.511}{3727.3}\ \frac{14.00\ \text{g/mol}}{7 \times 1.2 \times 10^{-3}\ \text{g/cm}^3} \times \frac{0.25}{2.86} = 3.2\ \text{cm}$$

Alpha particles are absorbed by a few centimetres of air (Fig. 5.24).

Solution to 5.5 From Eq. (5.41) we first calculate the average ionisation energy for aluminium: $I = 22.8 + 13 \times 9.7 = 149$ eV to be used in the average of the log term:

$$L = \ln\left(\frac{2 \times 0.511 \times 0.546\ \text{MeV}^2}{0.511 \times 1.49 \times 10^{-4}\ \text{MeV}^2}\right) = 8.89$$

we have:

$$R = 0.5 \times \frac{0.298\ \text{MeV}^2}{0.078\ \text{MeV}^2\ \text{cm}^2}\ \frac{0.511}{0.511}\ \frac{26.98\ \text{g/mol}}{13 \times 2.7\ \text{g/cm}^3} \times \frac{1}{8.89} = 0.33\ \text{cm}$$

The β particles from ^{90}Sr are stopped by a few mm of aluminium. In addition, they produce bremsstrahlung radiation, with end-point at 546 keV and characteristic K-lines of aluminium, at 1.6 keV. The low-energy X-rays from Al can be easily shielded either by aluminium itself or by a thin layer of shielding with higher Z. To shield at 99% from bremsstrahlung we can consider to use iron, with $\rho = 7.86$ g/cm^3 and $\mu = 0.084\,\text{cm}^2/\text{g}$.

$$-\mu' x = \ln(0.01) \Rightarrow x = 4.6/0.66 \approx 7 \text{ cm}$$

Bibliography and Further Reading

L. Cerrito, *Radiation and Detectors* (Springer International Publishing, Singapore, 2017)
A. Del Guerra, *Ionizing Radiation Detectors for Medical Imaging* (World Scientific, Singapore, 2004)
R. Fernow, *Introduction to Experimental Particle Physics* (Cambridge University Press, Cambridge, 1986)
G.F. Knoll, *Radiation Detection and Measurement* (Wiley, New York, 2012)
W.R. Leo, *Techniques for Nuclear and Particle Physics Experiments* (Springer, Berlin, 1993)
B.R. Martin, *Nuclear and Particle Physics - An Introduction*, 2nd edn. (Wiley, Chichester, 2009)
B. Povh et al., *Particles and Nuclei: An Introduction to the Physical Concepts* (Springer, Berlin, 2015)
E. Segré *Nuclear and Particle Physics* (W. A. Benjamin, Reading, 1977)
M.G. Stabin, *Radiation Protection and Dosimetry* (Springer Science+Business Media, New York, 2007)
S. Tavernier, *Experimental Techniques in Nuclear and Particle Physics* (Springer, Berlin, 2010)
J.E. Turner, *Atoms, Radiation, and Radiation Protection* (Wiley WCH, Weinheim, 2007)